From Large to Small, from Day to Night: The Sensory Costs of Miniaturisation in Ants

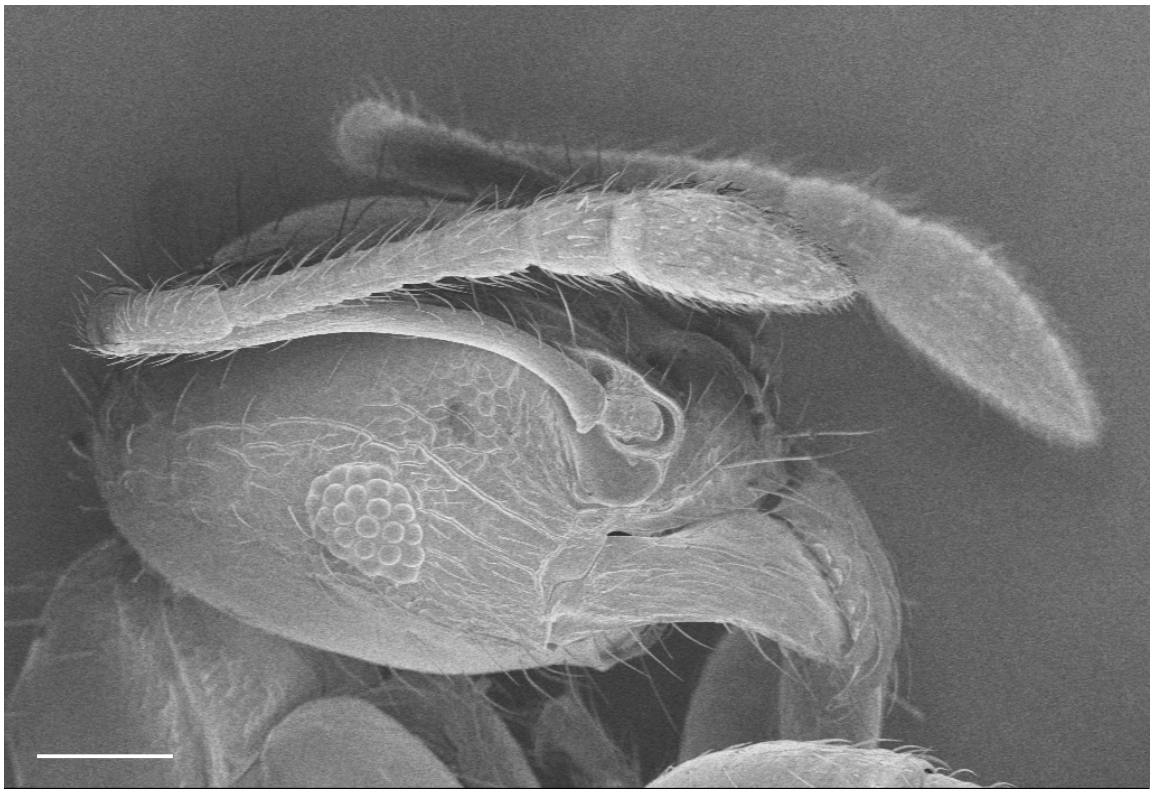

Fiorella C. R. Esquivel

Honours Thesis in Microscopy
Bachelor of Science (Adv.) (Hons.)
Australian National University
2012

Title page: Scanning electron micrograph of a *Pheidole sp. 1* minor worker. Scale bar = 100µm.

Declaration

Except where properly acknowledged the material presented in this thesis consists of original work resulting from research carried out between February and October 2012 at the Australian National University as part of my honours project in Microscopy. The work presented here has not been submitted in whole or in part for any other degree.

……

Fiorella C R Esquivel

25.Oct.2012

Acknowledgements

I am grateful to the Centre for Advanced Microscopy (CAM) at ANU for access to equipment and to their staff for training and assistance. I would like to thank Ajay Narendra and Jochen Zeil from the Research School of Biology as well as Melanie Rug from CAM for their help, support and supervision in all aspects of this project. Ali Alkaladi's advice in TEM sectioning and staining as well as in grid coating were absolutely invaluable. I would also like to thank Chloé Raderschall, Piyankarie Jayatilaka and Eliza Middleton for their encouragement and company throughout this project. Finally I would like to acknowledge the ARC Centre of Excellence in Vision Science for their generous scholarship.

Contents

List of figures:

Figure 22. Preliminary observations of the internal structure of the compound eye of the small *Pheidole sp. 1* major and minor workers.

Figure 23. Scaling of optical structures with body size and head width.

Figure 24. Optical cut-off frequency and resulting views that ants could possibly have.

1. General introduction:

Miniaturisation is the reduction of adult body size in a given lineage over an evolutionary timescale, where further reduction in size is not possible due to physical limits on the function of biological systems (Hanken and Wake, 1993). It is a fascinating phenomenon, common among diverse taxa including mammals, reptiles, amphibians, fish, foraminifera, annelids, crustaceans and insects and which has profound effects for all aspects of an animal's biology.(Hanken and Wake, 1993). Given its prevalence within the animal kingdom, miniaturisation must arguably confer significant evolutionary advantages. There are, however, costs associated with such dramatic reductions in body size: it is known that there are functional lower limits to neuron size (Eberhard, 2007) and there are restrictions to cell size imposed by a number of factors including the properties of lipid bilayer membranes, the structure of water and the volume needed for the function of macromolecules such as ribosomes (Pirie, 1973), as well as constraints imposed by the minimum size of a functional genome (Maniloff, 1996). In contrast, larger animals are able to afford larger structures which can be beneficial in some cases: (1) larger neurons with thicker axons reduce internal resistance and provide faster conduction of electrical potentials, (2) bigger brains offer animals more processing power (Chittka and Niven, 2009, Chittka and Skorupski, 2011) and (3) longer limbs result in faster locomotion (Christiansen, 2002, Wittlinger et al., 2007). Although it seems farfetched, even the size of an organism's genome can impact on its ability to evolve a reduced body size (Olmo, 1983, Roth et al., 1990).

In addition to the limits imposed by size, the time at which animals are active might also influence the design of sensory structures. Animals regularly operate in discrete temporal niches; this time partitioning is regulated by a variety of factors which includes competition from other animals, differences in predation pressure, and time-limited availability of food resources (Kronfeld-Schor and Dayan, 2003). Animals may, for instance, choose to avoid higher rates of predation by becoming crepuscular or nocturnal. However, being active during these temporal niches will mean that animals will have to face the challenge of carrying out their tasks in dim-lit and cooler conditions relative to diurnal animals. Day- and night-active animals are thus confronted with different demands on sensing and may thus require distinct sensory adaptations.

Given that miniaturisation operates on an evolutionary time-scale, it is very difficult to observe the process as it is taking place. A better approach to study miniaturisation would constitute studying an already established, diverse clade with species encompassing a large range of body sizes. This approach should enable comparisons between animals with derived miniaturised traits and non-miniaturised animals with ancestral traits to be drawn. Formicids are one such clade where individual species vary enormously in body size, going from 0.5 to 26mm in body length (Hölldobler and Wilson, 1990) making them ideal for the study of miniaturisation. Furthermore, worker polymorphism in ants provides a unique opportunity to compare the effects of decreasing body size within a single species. In addition, different species of ants are active at distinct times of the day, providing a range of diurnal-nocturnal ants which is essential to assess the effect of time of activity on the design of sensory structures.

Despite this variation in size and time of activity, the tasks that an ant must perform as part of life in a colony remain largely the same. Two of the most important tasks that worker ants perform are

communication among colony members and foraging, including the ability to navigate to a food source and back to the nest again. In order to perform these tasks ants must be able to obtain information from their environment. In the case of communication an ant obtains information mainly through chemoreception as most communication is performed through pheromone signalling (Ryan, 2002, Wilson, 1972). In the case of foraging many senses are involved but vision is of particular importance as most species depend largely on visual cues to navigate (e.g. Reid et al., 2011, Wehner et al., 1996). Hence, vision and chemoreception are not only interesting in the context of miniaturisation but are also crucial to the understanding of day to day tasks carried out by ants. Because many of the tasks carried out by worker ants are common across different species, comparisons between genera can be made. Additionally the study of these sensory systems in particular provides the opportunity to make reasonable predictions about the physical constraints and limitations governing their designs and, unlike more complex structures, they are amenable to quantitative analysis.

Although miniaturisation of the visual and chemoreceptive structures in ants has not been studied per se there have been a number of studies into the scaling of nervous tissue to body size. Previous studies focusing on insects have found allometric relations linking brain and body sizes (Cole, 1985, Rensch, 1948, Wehner et al., 2007). Furthermore, a recent study by Seid *et al.* (2011), built on a previous data set relating ant brain size to body size (Wehner et al., 2007) and found a diphasic allometry in brain volume when smaller ant species were included into the model. The first phase of the allometry was comprised of the previously known relationship which dictates the scaling of brain size in large ant species (> 0.9 mg body mass). The second phase applied to the brains of smaller species or castes (< 0.9 mg body mass) which scaled according to a different allometric relation. Small animals still had brain tissues which took up a great proportion of their body mass but this proportion was smaller than that predicted by the first phase of the allometry. Seid *et al.* (2011) argue that a reduction in brain size in small ants is unlikely to be a consequence of a size constraint within the head capsule as macrocephaly has evolved numerous times among the formicids (the *M. hirsutus* major workers studied here are an example of this). Instead it is hypothesised that the energetic costs of maintaining metabolically expensive nervous tissue may limit the size of brains and other nervous tissues in miniature animals (Niven and Farris, 2012, Niven and Laughlin, 2008, Niven et al., 2007).

Miniaturisation is evidently a promising field with many avenues of study yet unexplored. This thesis aims to make some initial forays into the miniaturisation of visual and chemoreceptive systems. First, suitable study species are identified and time of activity is established for each species by conducting field studies (Chapter 2). The effects of miniaturisation and time of activity on the design of specific components of the chemoreceptive (Chapter 3) and visual (Chapter 4) systems are then studied using a variety of techniques in microscopy. A final discussion compares the extent to which chemoreceptive and visual systems are affected by miniaturisation and time of activity, and the implications that this may have for different animals (Chapter 5).

2. Study species and determining activity schedules

2.1. Introduction

The size of an animal dictates a range of factors which define its unique ecological niche, including its position within a food web (Woodward et al., 2005), its thermal inertia (Hone and Benton, 2005) and the amount of nervous tissue available to it (Chittka and Niven, 2009, Chittka and Skorupski, 2011). Similarly, the time of day at which an animal is active also dictates the resources it has access to, the kind of predatory and competitive pressure it is under, and the range of temperatures and light levels it has to contend with (Kronfeld-Schor and Dayan, 2003, Schoener, 1974). To determine the effects of miniaturisation on sensory structures a comparative approach was taken which made it essential to study animals of different sizes and which are active at different times of the day.

2.2. Methods

Body size and activity patterns were studied across several ant species at the Campus Field Station, The Australian National University, Canberra. Of these initially observed ants, four species were chosen that best captured the variability in body size and activity time. Studying distantly related ants nicely complements ongoing work which addresses similar questions on sensory systems in closely related species within a single ant genus, Myrmecia (Narendra et al., 2011)

The four species studied were *Iridomyrmex purpureus* Smith (Formicidae: Dolichoderinae), *Melophorus hirsutus* Forel (Formicidae: Formicinae), *Notoncus ectatommoides* Forel (Formicidae: Formicinae) and *Pheidole sp. 1* (Formicidae: Myrmicinae).

2.2.1. Morphometrics

Body length (BL) and head width (HW) were recorded for all study species. For this I collected ants of each species and preserved them in 70% ethanol and carried out measurements from photographs of preserved specimens (viewed through a Leica Zoom 2000 dissecting microscope and photographed using a Canon Power Spot S50 digital camera with a custom made eyepiece adapter) or, in the case of head measurements, from SEM images showing a frontal view of the head (see Chapter 3 for details on imaging conditions). For body length, the entire length of the animal excluding the mandibles was measured. The widest distance along the head, usually posterior to the eyes, gave a measure of the head width.

2.2.2. Activity schedule

Nests for each of the study species were identified and monitored to establish activity patterns. For this a circle of 20 cm radius was marked using coloured pins and the number of ants entering and exiting this perimeter was recorded during a 24 hour period in ten minute bins. All activity patterns were determined over a single day using one focal nest for each species during the late summer month of March, 2012. All nests were located within the Campus Field Station, The Australian National University.

2.3. Results

Body size

Among the four species studied, two species (*I. purpureus* and *N. ectatommoides*) were monomorphic and exhibited very little variation in body size between individuals (Figure 1 A, Figure 2). In the other two species ants were either polymorphic (as in the case of *M. hirsutus*) or dimorphic (as in the case of *Pheidole sp. 1*). In such cases, where more than one worker caste was present, morphometric measurements were carried out on only the two extremes, the major and minor workers. Both the body length and head width of the largest ant *I. purpureus* (BL = 8.7mm, HW = 2.0mm) were nearly 5 times more than those of the smallest ant *Pheidole sp. 1* (BL = 1.7mm, HW = 0.4mm). Body length of the studied ants gradually increased among the six animals from *Pheidole sp. 1* minor to *I. purpureus*. Head size also exhibited similar general trends, with two notable exceptions. Though *N. ectatommoides* had a greater body length than *M. hirsutus* major, the head size of the former was surprisingly smaller than the latter. In general, body length and head width did not scale similarly. For example in *I. purpureus* while the body size was nearly 1.60 times more than *M. hirsutus* major, the head size increased only by 1.17 times.

Activity time

Of the four studied species, two were exclusively day-active (*I. purpureus* and *M. hirsutus*) and two were exclusively night-active (*N. ectatommoides* and *Pheidole sp. 1*) (Figure 1). The activity schedules for *Iridomyrmex purpureus* are adapted from Greenaway (1981), while I carried out 24-hr stretches of fieldwork to identify the activity pattern in the remaining three species. *I. purpureus* exhibited a bimodal activity pattern with outbound and inbound activity peaks about four hours after sunrise and another peak in activity just before sunset. The other diurnal species, *M. hirsutus,* also had a brief but intense activity but this time during daylight hours. This seemed to take place in the warmest part of the day, between 1:00pm and 4:00pm. The two strictly nocturnal species exhibited very distinct activity periods at night. *N. ectatommoides* began activity at about sunset time, and was active only for about 4 hours after sunset. *Pheidole sp. 1* began activity about 30 minutes after sunset, remained active throughout the night and stopped activity about one hour before sunrise.

Figure 1

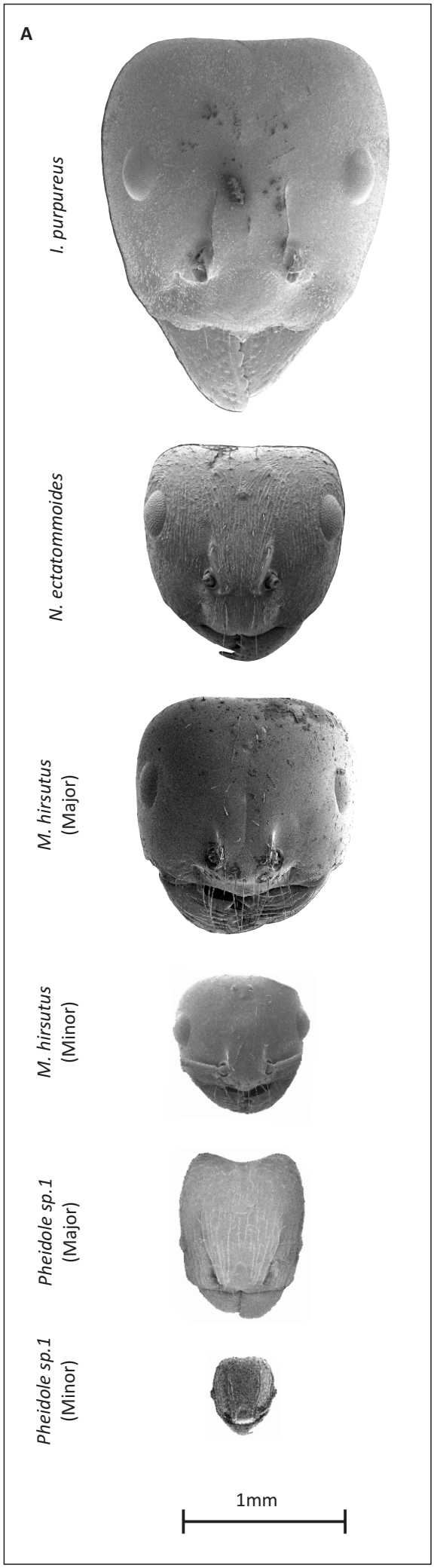
A
I. purpureus
N. ectatommoides
M. hirsutus (Major)
M. hirsutus (Minor)
Pheidole sp.1 (Major)
Pheidole sp.1 (Minor)
1mm

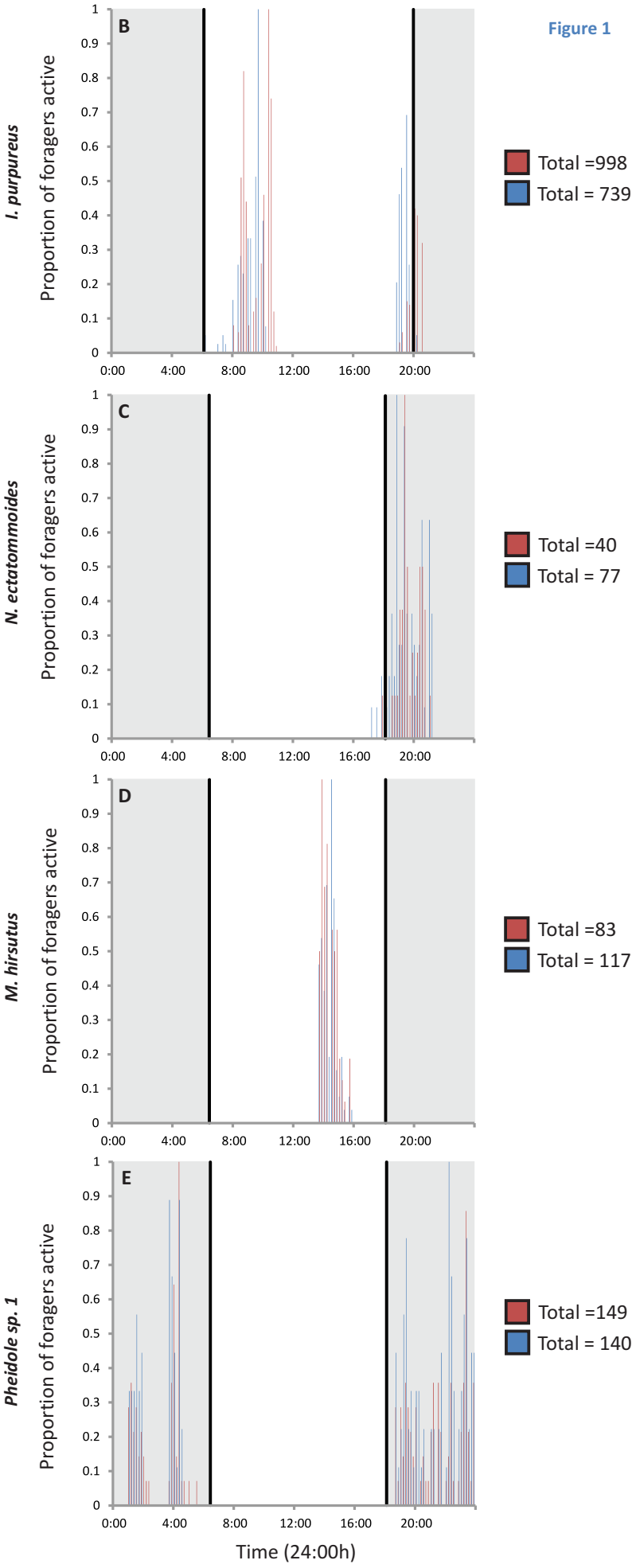
B
I. purpureus
Proportion of foragers active
Total =998
Total = 739
C
N. ectatommoides
Proportion of foragers active
Total =40
Total = 77
D
M. hirsutus
Proportion of foragers active
Total =83
Total = 117
E
Pheidole sp. 1
Proportion of foragers active
Total =149
Total = 140
0:00
4:00
8:00
12:00
16:00
20:00
Time (24:00h)
Inbound foragers
Outbound foragers
Day time
Night time

Figure 1

Summary figure showing **(A)** SEM images of the heads of the four study species (including major and minor workers) and **(B-E)** histograms showing their activity schedules. Figures **(C)** to **(E)** are based on results from original research while figure **(B)** has been modified from Greenaway (1981).

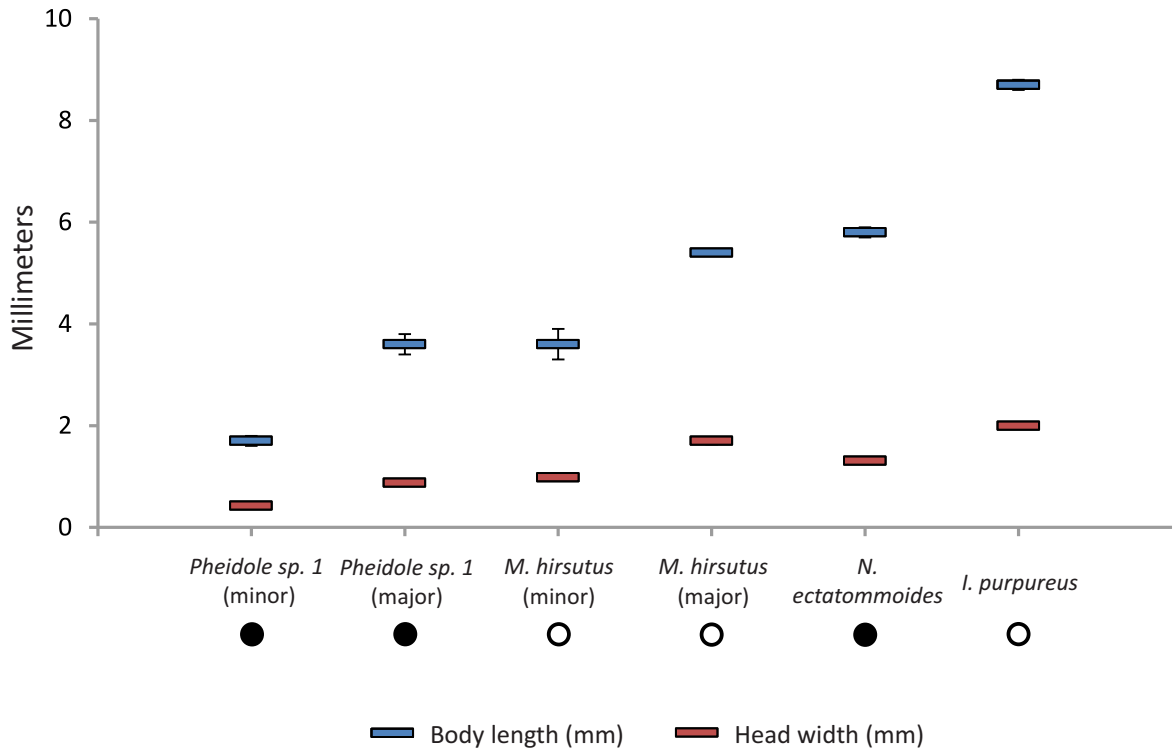

Figure 2

Morphometric measurements of the different species/castes of ants. Average body length (x̄±SE, n= 2 for each) and head width (x̄±SE, n= 5) are shown. Activity time of each species is shown: day-active (open circles) and night-active (closed circles). Note: errors bars in some cases may not be visible as the data is tightly packed.

There were two brief (60 minutes) interruptions in activity on the night *Pheidole sp. 1* was studied which corresponded to brief periods of fine drizzle.

2.4. Discussion

The size of an ant was determined by its body length (BL) and head width (HW). Both these measures are regularly used in myrmecology as reliable taxonomic criterions. The two sensory structures, the antennae and eyes, addressed in Chapters 3 and 4, are located on the head and the available surface area and volume could vastly limit their size and shape. Hence there was a need to determine the head size especially since it is evident that head size does not scale linearly with body size. In addition, major worker of *Pheidole* ants typically have disproportionately longer heads compared to minor workers, which is most likely to accommodate more adductor muscles for their large mandibles (Wilson, 2003). In such cases especially, a measure of head width offers a more reliable measure than body length.

The presence of major and minor workers in two of the study species provided the opportunity to study intraspecific size variations in addition to the changes observed between species. This also increased the number of animals being studied from four to six, especially relevant for the analyses of sensory structures.

Ants, like most other organisms, can be classified as diurnal, crepuscular and nocturnal. While some ants adhere to a fixed activity time throughout the year, in most species activity time is regulated by abiotic factors. Animals may tune their daily activity to factors such as light levels (Kotler et al., 1991, Kronfeld-Schor and Dayan, 2003, Narendra et al., 2010), temperature (Grubb Jr, 1978) or sunrise and sunset times (de Groot, 1983, Welbergen, 2008). In addition, biotic factors such as competition, predation and foraging style also influence activity schedules. Of the four species studied, two are strictly solitary foraging (*M. hirsutus*, *N. ectatommoides*) while the other two engage in both trail following and solitary foraging (*I. purpureus*, *Pheidole sp. 1*). The differences in activity patterns between the nocturnal *N. ectatommoides* and *Pheidole sp. 1* may be explained due to their different foraging styles. It was also observed that while both major and minor workers of *M. hirsutus* engaged in foraging behaviours only the minor workers in *Pheidole sp. 1* foraged while the major workers acted as soldiers.

A seasonal monitoring of activity patterns should reveal whether ants switch from diurnal to nocturnal lifestyle or vice-versa. However, given the time constraints and that the main aim was to identify suitable ants to pinpoint the sensory costs of miniaturisation, a one-time sampling for activity schedules was deemed suitable. From this single-day activity observations four species of ants were identified (two diurnal and two nocturnal) comprising six different body sizes. The variation in the sensilla and eyes of these species will be identified in the following chapters.

3. Antennal chemoreceptors

3.1. Introduction

When an ant is viewed under a high magnification microscope the presence of numerous hairs covering the external cuticle becomes immediately apparent. These hairs are sensory sensilla, self-contained sensory units consisting of modified cuticular structures which perform a variety of roles and are present in most insects. The shape of a sensillum depends on its function; not all sensilla are filiform, some may be dome shaped or sunken under the cuticular surface. Sensilla may be mechano- , chemo-, thermo- or hygroreceptive, or even be sensitive to changes in CO_2 levels (Altner and Prillinger, 1980, Kleineidam et al., 2000, Kleineidam and Tautz, 1996, McIver, 1975, Rutchy et al., 2009). Because of their important role in the day to day life of an ant, the focus of this study lies with chemoreceptive sensilla.

Structurally, sensilla consist of an external cuticular sheath which houses a primary sensory neuron and protects it from mechanical damage and desiccation. The neuron, or neurons, are enveloped by accessory cells, such as sheath, tormogen and trichogen cells (Eguchi and Tominaga, 1999, Ryan, 2002). These cells are responsible for the construction of the outer cuticular structure during development and ecdysis and also secrete receptor lymph fluid (Altner and Prillinger, 1980, Ryan, 2002). This fluid plays various roles which include preventing desiccation of the neuron in porous sensilla (such as chemoreceptors) and assisting neuron function and membrane potential maintenance (Altner and Prillinger, 1980). Furthermore, lymph fluid is vital to the normal functioning of chemoreceptors as it prevents continuous stimulation by removing and metabolising stimulus molecules (Ryan, 2002).

The gross morphology of sensory sensilla is shaped by the outer cuticular element and generally follows the same basic structure (Frazier, 1985). An outer hair, peg or other stimulus conducting structure is attached to a socket or protrudes through an opening in the cuticular surface (Altner and Prillinger, 1980). Some sensilla are found sunken within the antennal lumen but these still follow a similar general structure.

3.1.1. External morphology of known chemoreceptors

Although numerous types of sensilla are found in most insects, the antennae of ants have consistently been found to carry seven particular types of sensilla. These sensilla are: sensilla trichodea curvata, sensilla basiconica, sensilla trichodea, sensilla chaetica, sensilla coeloconica, sensilla ampullacea and sensilla campaniformia (Dumpert, 1972b, Hashimoto, 1990, Kleineidam and Tautz, 1996, Kleineidam et al., 2000, Renthal et al., 2003, Ozaki et al., 2005, Marques-Silva et al., 2006). Of these sensilla, there is evidence to suggest that the first three are involved in chemoreception either through direct contact with the substrate (contact chemoreception) or by intercepting volatile chemicals (olfaction) (Dumpert, 1972b, Dumpert, 1972a, Hashimoto, 1990, Ozaki et al., 2005, Renthal et al., 2003). This study aims to identify variations in the structure and distribution of these three chemoreceptors in ant species of different sizes which occupy different

temporal niches to pinpoint some of the possible constraints imposed by miniaturisation and time of activity on chemoreception. Although sensilla are found throughout the body (Figure 3 A), chemoreceptors are usually found on the antennae, labial and maxillary palps and sometimes on the tarsi (Altner and Prillinger, 1980). Of these, antennae hold the highest concentration of chemoreceptors; previous surveys of ant antennae have found particularly high densities of chemoreceptors on the apical segment (see Figure 18). Consequently the apical segment will be the focus of this study.

Information on the chemoreceptors of ants is available from a limited number of studies which have identified, described and surveyed the sensilla of different species of ants (Dumpert, 1972b, Hashimoto, 1990, Renthal et al., 2003). However, relatively little is known about the variability of chemoreceptors within and between species, or about differences in their distribution. While some studies have compared the numbers and types of sensilla found in worker and alate castes (Renthal et al., 2003, Dumpert, 1972b) there is very little information on how miniaturisation or time of activity may influence chemoreceptor presence, size or distribution. Nevertheless, good descriptions of the external morphology of sensilla trichodea curvata, sensilla basiconica, sensilla trichodea are available and these are outlined below:

Sensilla trichodea curvata (Figure 3 C-E)

These are bilaterally flattened sensilla which curve sharply near the base (Figure 3 C). Renthal *et al.* (2003) described a noticeable variation in width at the base (1.0-2.5 μm) and length (15-25 μm), within a single ant species (*Solenopsis invicta*), where the thinner sensilla tapered continuously to a sharp point while the thicker sensory hairs had a distinctive bevelled tip. They also identified the presence of pores leading into the lumen of the sensilla using a silver nitrate staining technique (Figure 3 D, E). The staining revealed pores along the lateral surface of the sensilla but not on the medial surface. This type of sensillum has been observed to occur in numerous formicids from across the phylogeny (Dumpert, 1972b, Hashimoto, 1990, Renthal et al., 2003). Based on the structure and distribution of sensilla trichodea curvata, Hashimoto (1990) and Renthal *et al.* (2003) attribute an olfactory function to this sensillum, while electrophysiological experiments by Dumpert (1972a) further support this hypothesis. To avoid confusion with sensilla trichodea, the sensilla trichodea curvata will be referred to from here on as simply sensilla curvata.

Sensilla basiconica (Figure 3 B)

These are filiform sensilla generally recognised by the conspicuously large socket surrounding the base of the sensory hair. It is also unusually thick relative to other filiform sensilla (e.g. sensilla chaetica and sensilla trichodea) and generally has a blunt tip (Figure 3 B, white arrow), although this is not always the case (Hashimoto, 1990, Ozaki et al., 2005). In contrast to the majority of sensilla which are angled towards the antennal tip, sensilla basiconica stand almost perpendicular to the cuticular surface (Renthal et al., 2003). Renthal *et al.* (2003) identified two types of openings on the sensillar surface: (a) pores, found along the tip and distal part of the sensillum, and (b) grooves, which ran along the rest of the sensillum. This led them to suggest that the sensilla may have a

double function as both an olfactory and contact chemoreceptor. Although, multiporous sensilla are usually associated with olfaction and not contact chemoreception (Steinbrecht, 1999) electrophysiological experiments on *Camponotus japonicus* have shown that sensilla basiconica respond to contact stimulation (Ozaki et al., 2005). More specifically, the study showed that the sensilla responded differentially to contact with nestmate and non-nestmate cuticular hydrocarbons (CHCs). Given that CHCs are non-volatile (Ozaki et al., 2005, Provost, 2008), all sensilla involved in nestmate recognition from CHC identification will act via contact chemoreception. Behavioural observations further support the case for sensilla basiconica as a contact chemoreceptor given that nestmate recognition generally occurs after antennation (Ozaki et al., 2005, Beugnon et al., 2001).

Sensilla trichodea (Figure 3 B)

These are long slender sensilla with blunt tips (Figure 3 B, black arrows). Silver nitrate staining in *Solenopsis invicta* has revealed the presence of pores throughout the sensillar surface (Renthal et al., 2003).

Sensilla basiconica and sensilla trichodea are often found in close association with one another (Hashimoto 1990; Kleineidam and Tautz 1996). Sensilla trichodea are often found placed distally to sensilla basiconica and, depending on the taxon, the partnered sensilla may be of equivalent or different sizes to each other (Esquivel, 2011, Renthal et al., 2003). Given this paired organisation it has been suggested that formicids may use these sensilla to compare the different properties of a chemical stimulus (Renthal *et al.* 2003).

3.1.2. Design limitations in chemoreceptors

Miniaturisation

Insect chemoreception has been a subject of interest for many years now with numerous studies covering a variety of different aspects from the anatomy of receptors (Altner and Prillinger, 1980, Hashimoto, 1990, Zacharuk, 1980) to the mechanisms of chemical binding, signal transduction and amplification (Hansson and Stensmyr, 2011, Ryan, 2002, Wicher, 2012). However, specific design constraints have not been clearly identified for the construction of insect chemoreceptors, particularly under the conditions of miniaturisation that this thesis will focus on. A general review of chemoreception across a variety of taxa by Wicher (2012) gives an indication of the kind of physical and morphological factors which may have an impact on chemoreception. For molecules to be perceived, they must interact with membrane receptors, either in the cell membrane of a single-celled organism or in the membrane of a dendrite in a multi-cellular organism. It thus follows that the larger the surface area available the more likely this interaction will take place. A large surface area should thus ensure accuracy, as the probability of perceiving a given molecule becomes proportional to the concentration of the odour molecule in the medium (e.g. air or water). Accuracy is an important characteristic of a chemoreceptive system as animals use the difference between previously and currently experienced odour concentrations to perform chemotaxis (e.g. travelling along chemical concentration gradients or tracking turbulent odour plumes) (Vickers, 2000)

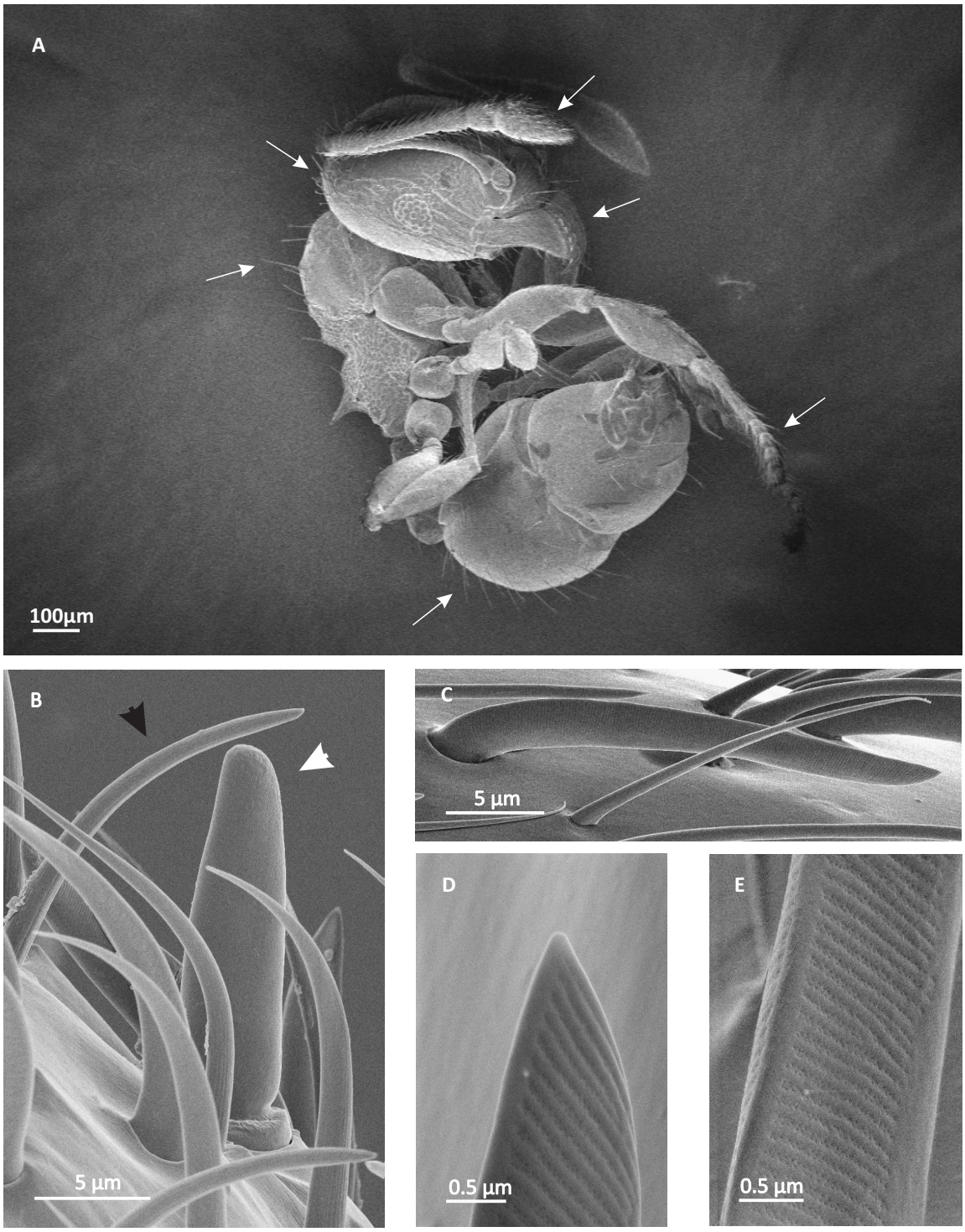

Figure 3

Scanning Electron Micrographs (SEM) of ant sensilla. **(A)** The smallest ant studied *Pheidole sp. 1* minor worker. Arrows indicate location of sensilla on the antennae, mandibles, head, thorax abdomen and legs. **(B)** Example of two sensilla on the largest ant studied *Iridomyrmex purpureus*, sensilla trichodea (black arrow) and sensilla basiconica (white arrow). **(C-E)** Example of sensilla curvata in *Pheidole sp. 1* minor. **(C)** Shows sensilla curvata in profile view and **(D,E)** shows the sensillum tip and shaft with transverse rows of pores.

Increasing the probability of interaction decreases the detection time and increases the accuracy of the system that is, the proportion of times a molecule will be perceived relative to the number of times it is encountered. A landmark study into bacterial chemotaxis (Berg and Purcell, 1977) developed an equation which put all these factors into context. Thus the fractional accuracy in determining concentration (c) of a chemical stimulus is determined by:

$$\delta c/c = 1 / \sqrt{D r c_m t}$$

where: D = diffusion coefficient of stimulus molecule

r = receptor radius

c_m = concentration of stimulus molecule

t = detection time

In other words, given a stimulus of equal strength (concentration) and diffusivity animals with larger chemoreceptors will perceive a change in concentration of the stimulus molecule closer to the actual concentration than animals with smaller receptors over a given period of time. Alternatively, animals with smaller receptors will require a longer period of time to obtain an equivalent level of accuracy. This formula applies to single receptors or a receptor array, although an additional term describing the number and spacing of receptors in the array is necessary when considering the latter scenario. This concept can be generalised to organisms of different sizes. However, as the active space of an organism (i.e. the space in which it interacts) becomes larger and more complex, additional factors will come into play making it increasingly harder to reliably predict detection times and the fractional accuracy of a given receptor. Furthermore, in the original context stimulus molecules interact directly with receptor proteins without having to negotiate entrance into the lumen of a sensillum. Therefore, the number and size of pores a sensillum possesses will affect sensitivity by either allowing or restricting the diffusion of molecules into its lumen. Conversely large, numerous pores may cripple the function of a chemoreceptor by facilitating evaporation of the receptor lymph fluid. It is apparent that the size of a receptor will be of major importance as it will determine its ability to produce and store sufficient lymph fluid and the amount of surface area available will dictate the number and size of pores that may be present.

Time of activity

There is little reason to believe that differences in light intensity might affect the design of chemoreceptors. However, higher temperatures during the day may lead to desiccation of the internal structures which may drive the emergence of adaptations to prevent this. Such adaptations may consist of somehow making sensilla less exposed or reducing the size and/or number of pores on their surface. To the best of my knowledge, there have been no reports of this kind of adaptations in insect sensilla.

3.2. Methods

The external morphology of the antennal chemoreceptors was studied using scanning electron microscopy (SEM). Live specimens were collected and immersed directly in 50% ethanol for preservation. Whole heads or detached antennae were mounted onto aluminium stubs using adhesive carbon tape ensuring that the antennae were flat down with the dorsal surface facing upwards. A significant amount of time was invested into developing SEM protocols and quantitative methods for this section as a standardised procedure for the study of antennal sensilla had not been established at the time of this study.

Low magnification imaging

The distribution and size of sensilla were studied in the apical segment of the antennae using low magnification (x 1,500) serial images from five individuals of each species and caste. These SEM images were collected using a Hitachi S-4300 SE/N FESEM and later stitched using CorelDRAW® Graphics Suite X5 (2010 Corel) to obtain a detailed image of the entire segment. The nature of this work required a large depth of field so the smallest available aperture was used. To compensate for the resulting limit on illumination a large working distance was used (WD ≈ 12mm) and samples for this work were coated relatively thickly with Au/Pd (20mA, 4 mins). This permitted the use of higher accelerating voltages (5kV) without charging or damaging the sample.

Using these images the distribution of sensilla was mapped in a Matlab (2007a Matworks Natick, Massachusetts) based program Digilite (Jan Hemmi and Robert Parker, Australian National University). The maps were then used for a comparative analysis of the intra- and interspecific variation of sensillar distribution.

Measurements of the sensilla and apical segment length were carried out using ImageJ 1.45s (Wayne Rasband, National Institutes of Health USA). Length, diameter and 2D area were measured in at least five sensilla of each type in each specimen, ensuring that the measurements were for sensilla from different areas of the apical segment (see Figure 4 for details). Measurements were taken only using sensilla which were clearly imaged in full profile. Sensilla which were imaged at an angle, pointing away from or towards the 'camera' were ignored. This ensured that the measurements taken were representative of the true dimensions of the sensilla, but severely limited the number of sensilla. In addition, the distance from each individual sensillum to the apex of the segment was also recorded together with morphometric measures of body length (BL) and head width (HW).

High magnification imaging

Each of the three types of sensilla in each species/caste was imaged at high magnification (x ≥10,000) for description and qualitative comparison. Given the high level of detail necessary for this, samples were thinly coated with Au/Pd (20mA, 2 mins) and imaged using a Zeiss UltraPlus FESEM at 3kV using an intermediate aperture and a working distance of ~3mm. Images were edited using CorelDRAW® Graphics Suite X5 (2010 Corel). Contrast, colouring and cropping were the only image properties modified.

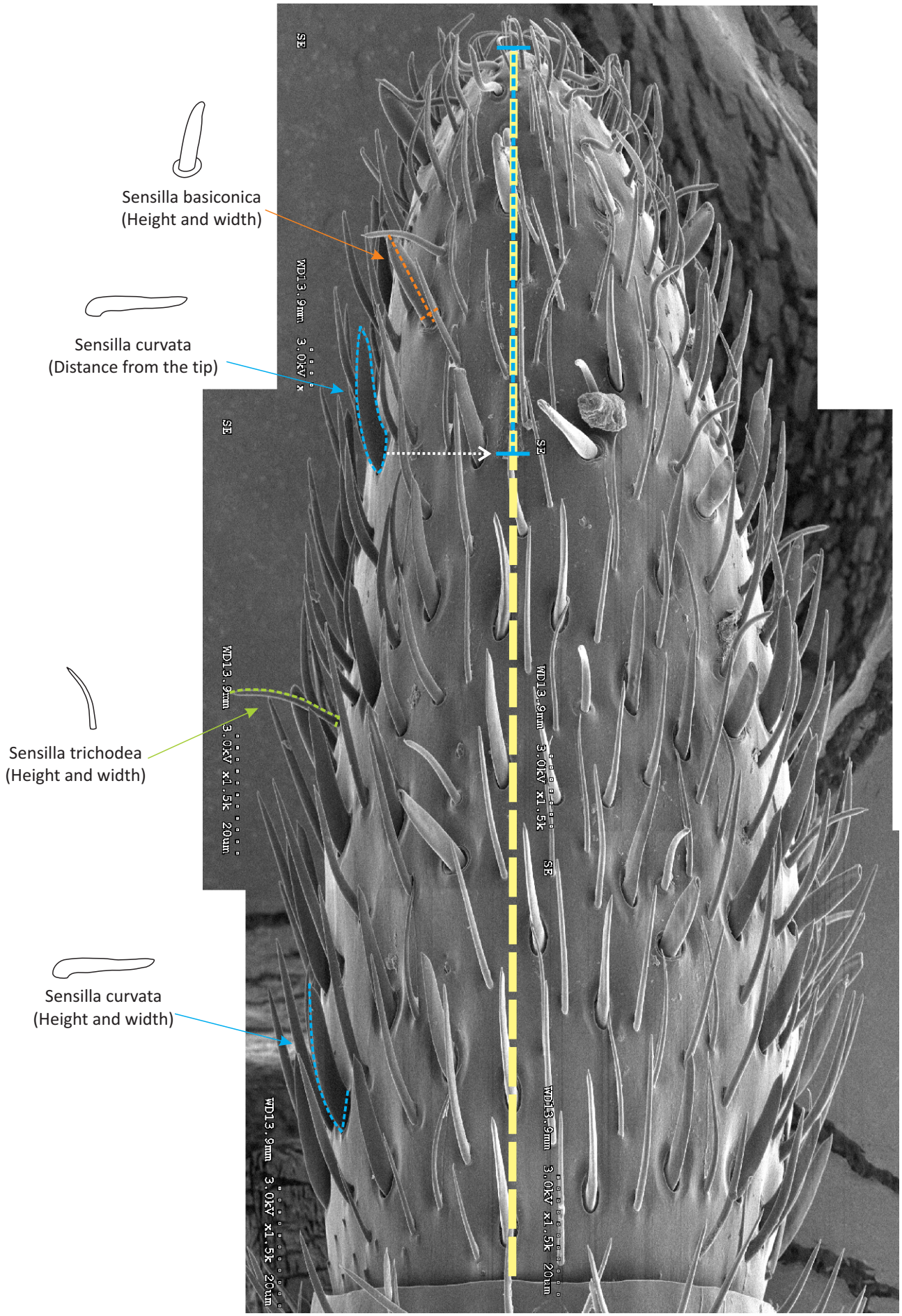
Sensilla basiconica
(Height and width)
Sensilla curvata
(Distance from the tip)
Sensilla trichodea
(Height and width)
Sensilla curvata
(Height and width)
SE
WD13.9mm 3.0kV x1.5k 20um

Figure 4

Example of an apical segment map (M. hirsutus minor worker) showing how sensillum measurements were taken. 2D area was measured by tracing the outline of a sensillum in profile (see sensilla curvata in blue) while the distance from the tip was determined by tracing a line from the middle of the base of the sensillum up to a line running from tip to base down the middle of the apical segment (black dotted line) and then measuring the distance from there to the tip (see blue dotted line). The length of a sensillum was measured either by tracing a curved line along its length (s. trichodea in green and curvata in blue) or by measuring in a straight line from tip to base (s. basiconica in orange). Sensillum widths were measured at the base (blue, green and orange dotted lines).

3.3. Results

3.3.1. Abundance and distribution of sensilla

The three sensilla studied occurred in similar proportions across the four species and each sensillum had a distinct distribution across the apical segment which was conserved across species (Figure 5 A and C). Sensilla basiconica and trichodea occurred either individually or paired. Of these two receptors sensilla trichodea were more abundant (they made up 29-34% of studied chemoreceptors) than basiconica (15-24%) and thus occurred individually with a much higher frequency. The unpaired sensilla trichodea were found throughout the apical segment but most notably in a small area around the tip where they were present in high densities. Only sensilla trichodea and filiform mechanoreceptors were observed in this area (see Figure 5 B and C). Sensilla trichodea and basiconica were most abundant in the distal four fifths of the apical segment (Figure 6). Sensilla curvata were the most abundant of all three sensilla (44-56% of chemoreceptors) and occurred in highest numbers lower down the apical segment in the proximal four fifths, with the last fifth containing almost exclusively sensilla trichodea and filiform mechanoreceptors (see Figure 5 and Figure 6; an example of a mechanoreceptor may be seen in Figure 5 B). This was the case across animals of all sizes.

The largest animals had the most chemoreceptive sensilla. When comparing absolute numbers the abundance of sensilla gradually increased from the smallest ant *Pheidole sp. 1* minor workers to the largest, *I. purpureus* (Figure 5 A). The only exception to this trend was *Pheidole sp. 1* major workers which had a reduced number of sensilla. When the number of sensilla was scaled to body length, head width and apical segment area, the relation fluctuated in strength according to the size metric used (see Figure 7). Variation in sensilla number between animals was best explained by the variation in apical segment size instead of body length or head width (Figure 7). This was interesting as it indicates that the area of the apical segment does not scale with head width as directly as one would expect (Figure 9 B, R^2=0.65) although the relation is stronger in the case of body length (Figure 9 A, R^2=0.86). With the exception of *Pheidole sp. 1* major workers night-active animals had larger apical segment areas (Figure 9 C) and relatively more sensilla than expected for their size (Figure 7). Irrespective of the metric used *Pheidole sp. 1* major workers had consistently less sensilla than both the similarly sized *M. hirsutus* minor workers and the much smaller *Pheidole sp. 1* minor workers (Figure 7).

Larger animals tended to possess larger sensilla but this was not a simple linear relation (Figure 8). Regardless of the size metric used *I. purpureus* consistently exhibited smaller sensilla than would be expected for such a large animal under a simple linear model. Furthermore, this trend was only observed in sensilla basiconica and trichodea. Sensilla curvata, on the other hand, exhibited no clear pattern of scaling with body size: sensilla seemed to remain fairly constant in size across all species. *Pheidole sp. 1* major workers had the most variable sensillum sizes (Sensilla basiconica range = 52µm², sensilla trichodea range = 26µm², sensilla curvata range = 48µm²) closely followed by *N. ectatommoides* while *M. hirsutus* and *Pheidole sp. 1* minor workers had some of the least variable sensilla (Sensilla basiconica range = 31 µm² (*M. hirsutus* major), sensilla trichodea range = 10µm²

(*Pheidole sp. 1* minor), sensilla curvata range = 30µm² (*M. hirsutus* minor)). Sensillum sizes seemed to be quite variable within each species.

This variation in sensilla size within species and within individuals can, at least in part, be explained by the position of the sensilla on the apical segment: i.e. the distance of sensilla from the tip of the apical segment. Sensilla in most species typically appear to become smaller at the tip (Figure 10). The size decrease varied between species and this relation was exaggerated in *Pheidole sp. 1* (major and minor workers). Sensilla curvata tended not to scale so strongly (Figure 10), if at all, because they generally occurred further down the antenna away from the tip (Figure 6).

3.3.2. Morphology and dimensions of sensilla

Sensilla basiconica

In most species these sensilla were short and stout with numerous pores perforating the blunt tip and, to a lesser extent, the dorsal region (**Figure** 11, Figure 12). These sensilla protruded from the antennal surface at a much more obtuse angle than most sensilla, which caused them to frequently project above other sensory hairs. A further feature characteristic of sensilla basiconica was their insertion. Rather than inserting directly into the antennal cuticle, sensilla basiconica inserted into a thick round ring of cuticle found around the base of the sensilla. This feature was less prominent in *Pheidole sp. 1* than in the other species **(Figure** 11**)**.

There were considerable differences in the size of sensilla basiconica across different species (Figure 17 A), but not between individuals of the same species (Figure 17 A).

The large *I. purpureus* had the shortest sensilla (ranging from 8.9 to 17.1µm) while *Pheidole sp. 1* major workers had the longest (ranging from 12.8 to 31.5µm). However, it is important to note that most species, particularly the night-active *N. ectatommoides* and *Pheidole sp. 1,* exhibited a large range of sensillum lengths. All species had a similar and overlapping spread of sensillum widths with one exception: *Pheidole sp. 1* (major and minor workers). Both worker castes of *Pheidole sp. 1* had the narrowest (1.3 to 3.3 µm) sensilla compared to other animals (for instance *I. purpureus* ranged from 3.1 to 5.2µm), (see Figure 17 B). Interestingly, unlike in the two *M. hirsutus* castes, there was a considerable difference between the *Pheidole sp. 1* majors and minors. The majors had considerably longer, wider sensilla than the minors. Similar trends were observed with sensilla trichodea (Figure 17 D) but not in sensilla curvata (Figure 17 E). In the latter case the lengths and widths of the sensilla of all species were much more tightly clumped and the differences between species were much less marked.

Within all studied species there was variation in the size but not in the shape of sensilla basiconica, except in *Pheidole sp. 1.* In this, the smallest species, the shape of the sensilla varied with size (see Figure 13) and the range of sizes observed was exceptionally large (see Figure 17 B). The longer sensilla were thinner and almost completely straight along their length, while shorter sensilla were broader, narrowed around the middle and had broader tips. In all other species the proportions of the sensilla scaled with size.

There was no marked variation in sensilla number and distribution between day- and night-active animals. However the sensilla basiconica of night-active species tended to be longer (see Figure 17). Both day-active species (*I. purpureus* and *M. hirsutus*) had fine striations running the length of the sensillum which were absent in the night-active species (*N. ectatommoides* and *Pheidole sp. 1*) (Figure 12). There was no obvious indication that any of the anti-desiccation adaptations predicted, such as smaller pores of a reduction in the number of pores, were present in the sensilla studied. Day-active species in fact possessed a larger number of openings (both pores and striations) than night-active animals (see Figure 12). However, the quantitative study of the size and number of pores per sensillum proved to be outside the scope of this study. The level of magnification required to study the pores of sensilla was such that it rendered imaging conditions extremely difficult. Samples were often damaged from the heat generated by the high voltage electron beam. This meant that acquiring images in which pores were visible became very labour and time intensive, requiring special treatment of samples and having a high failure rate. These conditions obviously do not lend themselves to the compilation of large data sets. Alternative techniques, such as the silver nitrate stain used by Renthal *et al.* (2003) to provide contrast between pores and sensilla under a light microscope, may prove more fruitful in determining the number of pores per sensillum if not their size.

Sensilla trichodea

These sensilla are straight, slim and filiform, with a simple insertion into the cuticular surface with no socket (see **Figure** 11 black arrows, Figure 13 A inset). Similarly to sensilla basiconica they protruded at an angle of almost 90° from the cuticular surface. All species except for the smallest (*Pheidole sp. 1*) had striations on the surface of these sensilla but these followed different patterns and spacings (Figure 12 F-J). The tip of these sensilla varied from a sharp, "pinched" tip (*N. ectatommoides*, *M. hirsutus* major and minor) to a blunt tip (*I. purpureus, Pheidole sp. 1* major and minor) (Figure 12). The presence of pores on sensilla trichodea observed in other studies (Esquivel, 2011, Renthal et al., 2003) could not be confidently established due to the extremely small size of these pores. There was no variation in the size of sensilla between individuals of the same species and caste (see Figure 17 C). The length and width distribution followed similar trends to those seen in sensilla basiconica but the hair widths distribution was narrower (see Figure 17 D). A tendency for these sensilla to become somewhat curved towards the tip of the antenna was observed. This was less pronounced in most species but in *M. hirsutus* (major and minor workers) sensilla trichodea became practically 'S' shaped at the tip (see Figure 14 B).

Sensilla curvata (sensilla curvata)

These sensilla displayed the least morphological variation. The medium sized *N. ectatommoides* and *M. hirsutus* majors, as well as the small *M. hirsutus* minor, had very similar sensilla curvata (see Figure 15 B, C, D). Observations indicated that in both species the tip was bevelled, but with a sharp extension of the top margin, and the sensilla widened gradually towards the insertion throughout the length of the sensillum. The sensilla curvata of both species also had similar lengths and widths with somewhat wider sensilla seen in *N. ectatommoides* (see Figure 17 F).

In contrast, although their body sizes were the most different, sensilla curvata in the large *I. purpureus* and small *Pheidole sp. 1* were most similar to one another in shape. These species exhibited the greatest degree of variability in sensillar morphology with *Pheidole sp. 1* being the more extreme (see Figure 16, Figure 17 F). In both cases there seemed to be continuous variation from an elongated, slender form of the sensillum through to a shortened, stout form. The stout forms of both species had blunt tips with soft edges in place of straight margins and sharp angles (Figure 16 B and D). However, while the tips of the slender sensilla curvata of *I. purpureus* resembled those of *N. ectatommoides* and *M. hirsutus* (major and minor workers) described above those of *Pheidole sp. 1* were bevelled but without the sharp protrusion of the top margin (Figure 16 A and C). The slender forms of both species also had a fairly constant width throughout the length while the stouter forms broadened towards the base like *N. ectatommoides* and *M. hirsutus.* In addition, while the range in the lengths of sensilla curvata was great in both (*I. purpureus* = 13.9µm and *Pheidole sp. 1* = 13.0µm in majors and 11.3µm in minors) the smaller species had much longer sensilla (34.7 – 21.7 µm in majors and 32.9 – 11.3 µm in minors) than the larger *I. purpureus* (29.3 – 15.4 µm).

All species exhibited rows of pores which ran transverse to the length of the sensillum (see Figure 3 C and D, Figure 16). These pores ran from the tip to the insertion of the sensillum into the antenna with the rows sometimes becoming narrower just before the insertion. The number of pores and whether or not every pore leads to a dendritic segment is not yet known. Finally, it was observed that there was a trend for the pores of sensilla curvata of *Pheidole sp.* 1 to cover a larger proportion of the width of the sensilla. This, however, was not quantitatively confirmed.

No major morphological differences were observed between day- and night-active species except for the absence of striations on the sensilla basiconica of night-active species.

3.4. Discussion

Irrespective of size and time of activity, all of the studied species possessed the three focal chemoreceptors: sensilla trichodea, basiconica and curvata. The three sensilla occurred in similar proportions and distributions across all species irrespective of size or time of activity. This seems to indicate that all four species have similar chemoreceptive requirements or at least may employ their sensilla in a similar fashion. The number of sensilla seemed to scale more closely with body length than with head width (Figure 7 A, D, G and B, E, H). However, the main factor influencing the abundance of sensilla was the apical segment area (Figure 7 C, F, I). Interestingly, apical segment area scaled did not scale body length as closely as might have been expected (Figure 9). It seems to indicate that there are adaptive pressures leading certain ants to increase the size of their antennae relative to their body size. The size of chemoreceptors tended to increase with size irrespective of the metric used (i.e. body length, head width or apical segment area) with the exception of sensilla curvata (Figure 8). Size of sensilla did not scale with body size because of the large amount of variation. The smallest ant studied, *Pheidole sp. 1* showed a number of irregularities compared to the other ant species in terms of the variability in the size and shape of its sensilla.

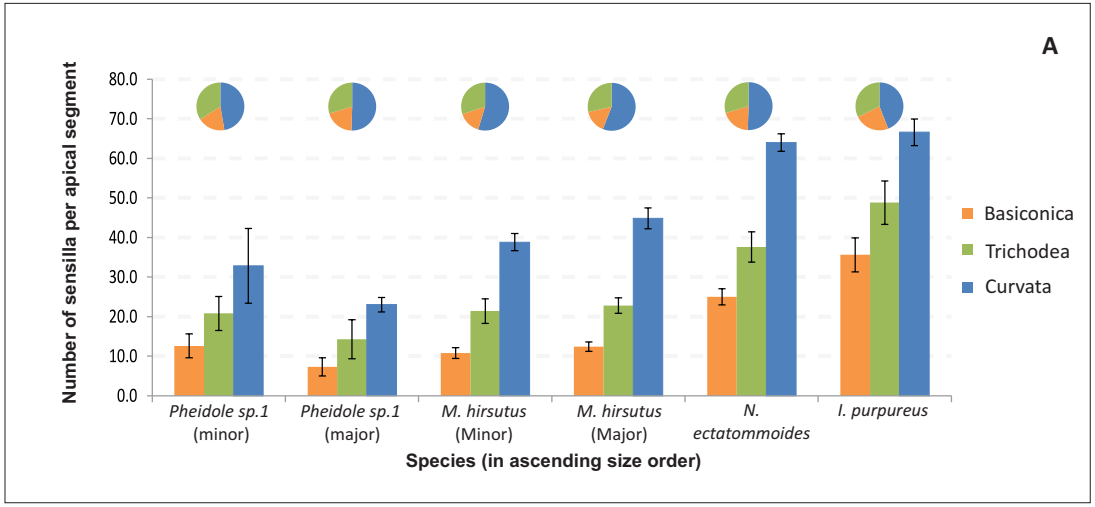

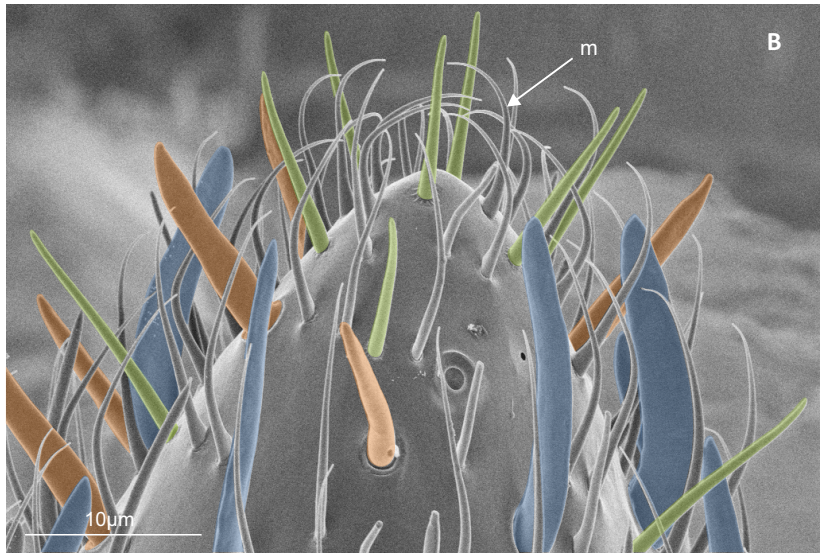

Figure 5

Overview of size and distribution of the three chemoreceptive sensilla in the apical segment of ant antennae. **(A)** Histogram of the average number of sensilla ($\bar{x} \pm SE$, n=5) in the apical segment. Pie charts represent the proportion contributed by each chemoreceptor sensilla. **(B)** SEM of the antennal tip of a *Pheidole sp. 1* minor worker showing sensilla curvata (blue), sensilla trichodea (green) and sensilla basiconica (orange). Sensilla at the tip of the antennae comprises of only trichodea (green) and mechanoreceptors (indicated as 'm'). **(C)** Distribution of sensilla curvata (blue triangles), trichodea (green squares) and basiconica (orange circles) on the apical segment of the antennae (images are to scale). The numbers of sensilla and distribution are based on images of a single individual of each species and caste and provide only an estimate of the average distribution. Day-active species: top row; night-active species: bottom row.

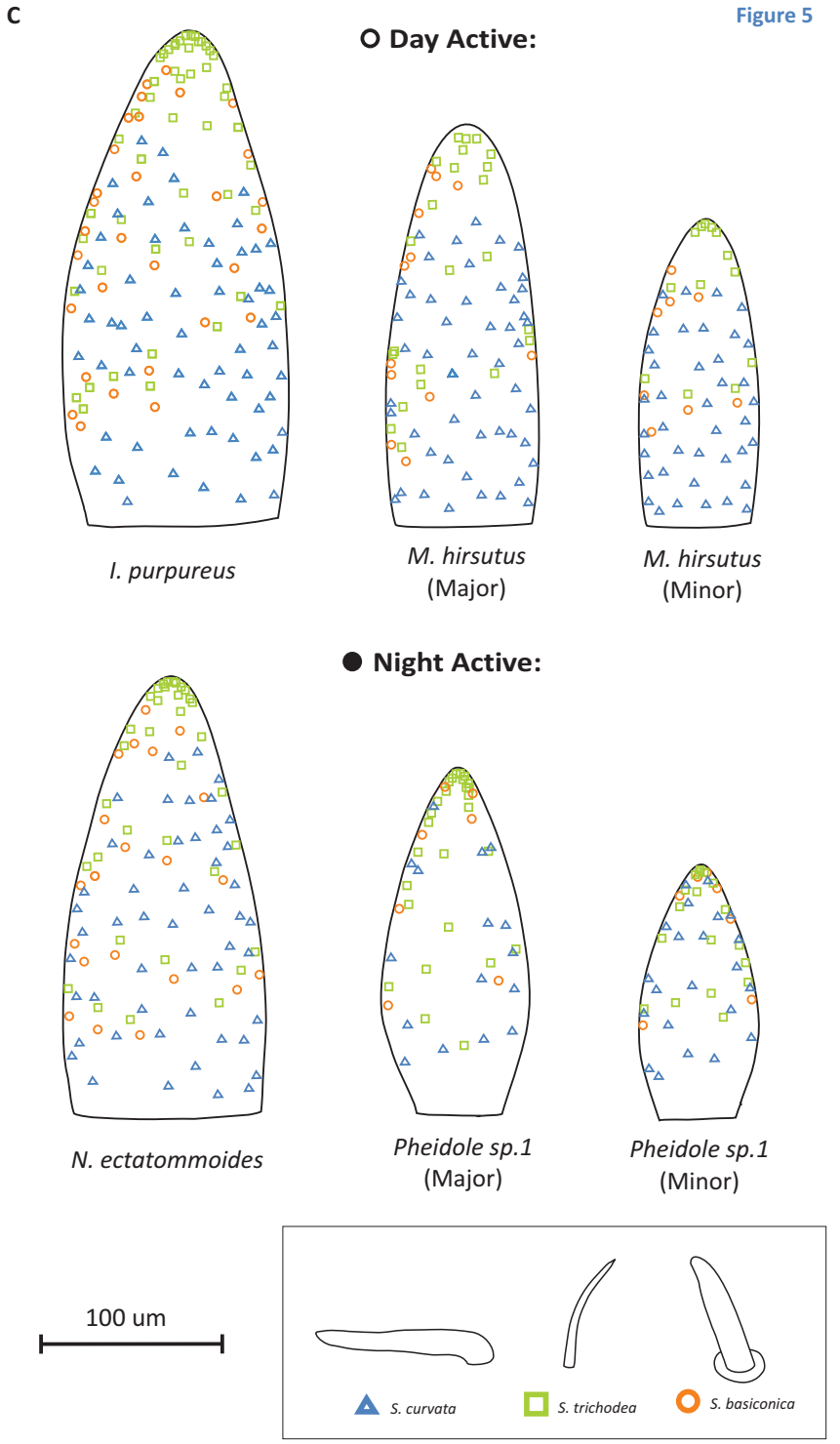

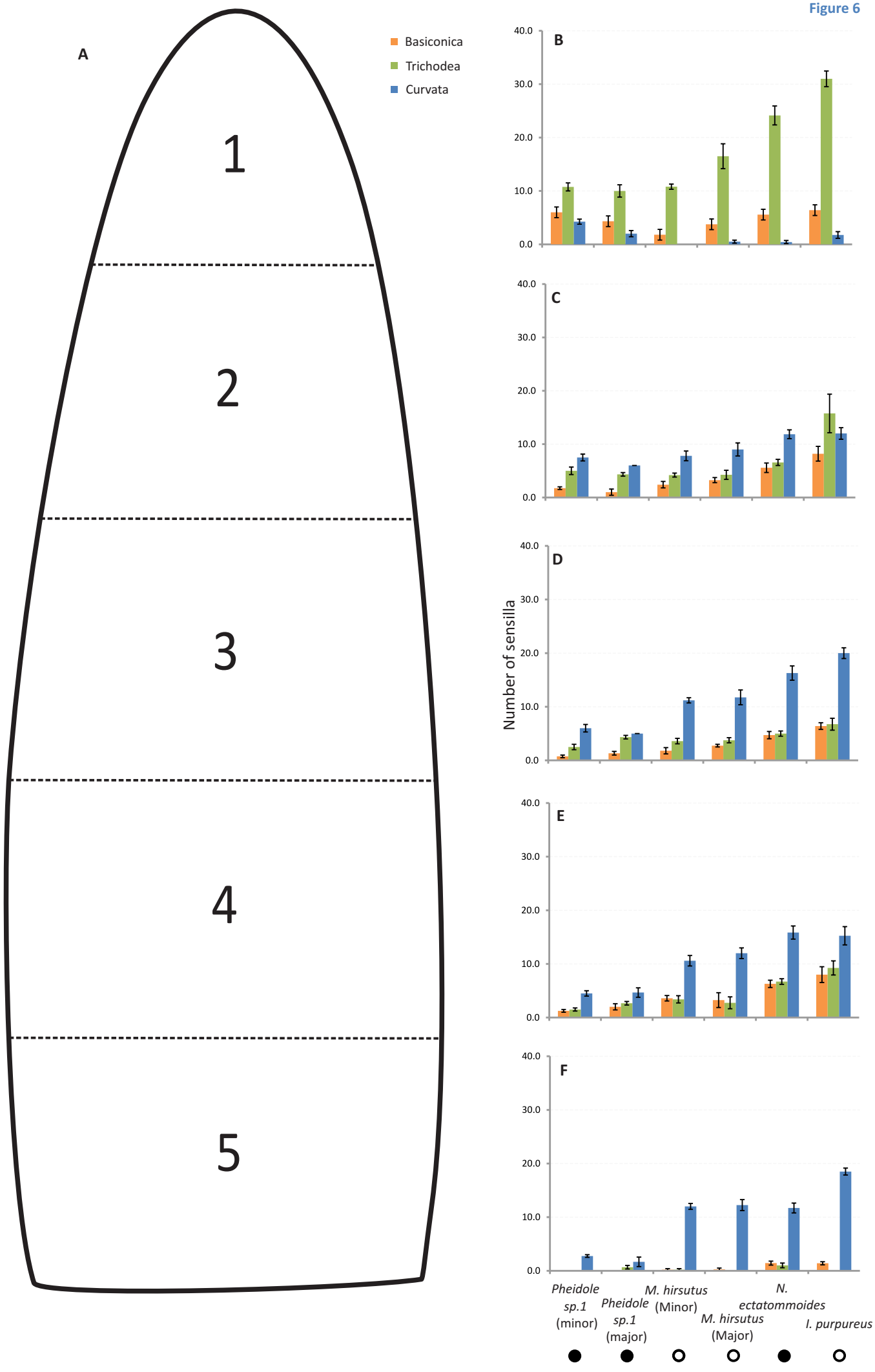
A
Basiconica
Trichodea
Curvata
1
2
3
4
5
B
C
D
E
F
40.0
30.0
20.0
10.0
0.0
Number of sensilla
Pheidole sp.1 (minor)
Pheidole sp.1 (major)
M. hirsutus (Minor)
M. hirsutus (Major)
N. ectatommoides
I. purpureus

Figure 6

Distribution of different types of chemoreceptors along the length of the apical segment. **(A)** Diagrammatic representation of the portion of the antenna surveyed for each accompanying histogram on the right, the length of the apical segment was divided into five equally spaced segments resulting in the five portions seen (numbered from the tip). **(B to F)** histograms showing the number of sensilla ($\bar{x}$ ± SE, n=4) in each of the adjacent portions of the apical segment.

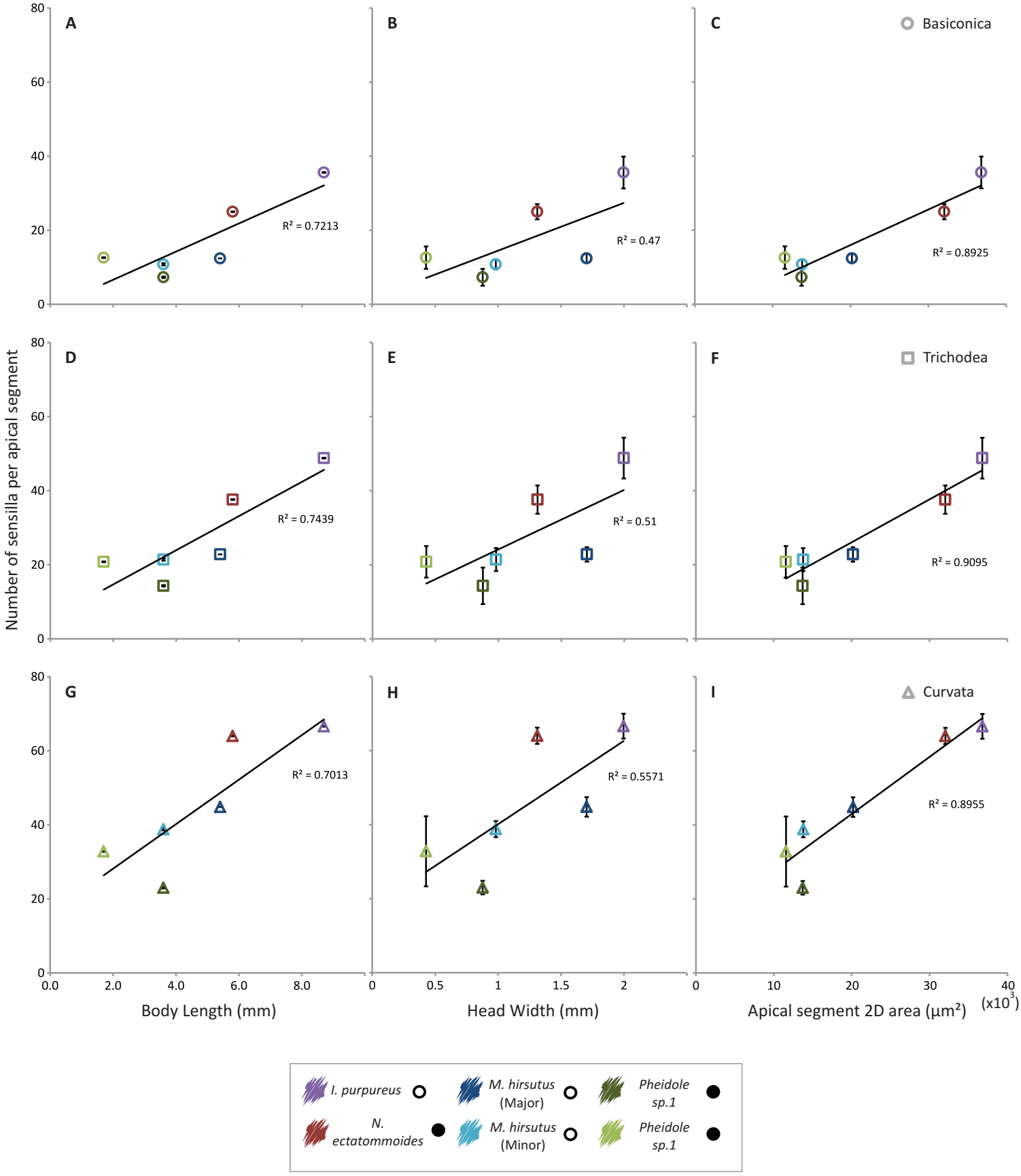

Figure 7

The relation between the number of chemoreceptive sensilla and the size of animals. Top row: sensilla basiconica; middle row: sensilla trichodea; bottom row: sensilla curvata. Average number of sensilla per apical segment (n= 4 to 5, x̄±SE) relative to: **(A,D,H)** body length, **(B,E,H)** head width and **(C,F,I)** apical segment area. Regression line is indicated by continuous black line. Day-active (open circles) and night-active (closed circles) ants are indicated.

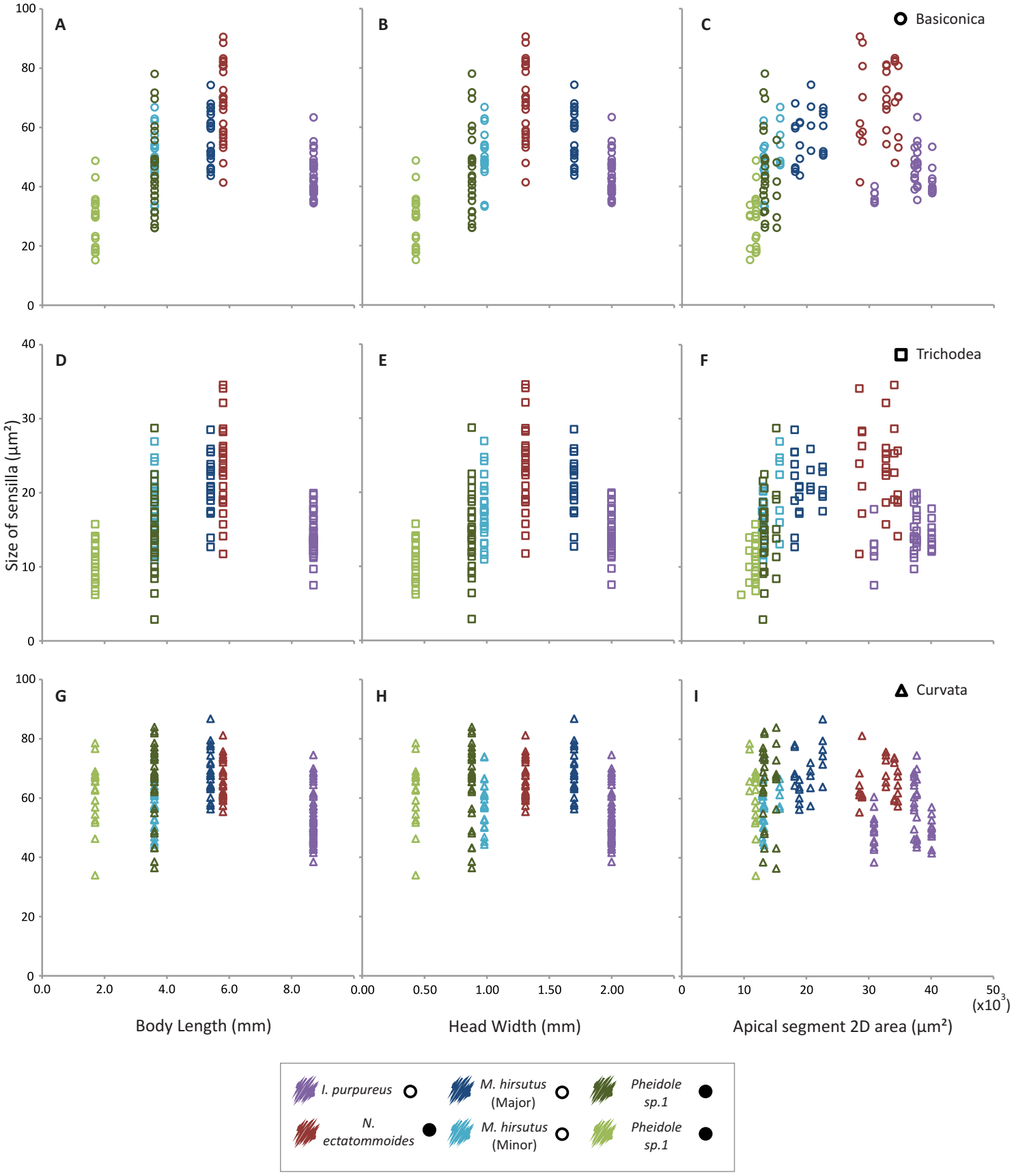

Figure 8

The relation between the size of chemoreceptive sensilla and the size of animals. Top row: sensilla basiconica; middle row: sensilla trichodea; bottom row: sensilla curvata. Absolute size of the sensilla relative to: **(A,D,H)** body length, **(B,E,H)** head width and **(C,F,I)** apical segment area. Note the change in y-axis labels in the middle row to display the comparatively smaller sensilla trichodea. Day-active (open circles) and night-active (closed circles) ants are indicated.

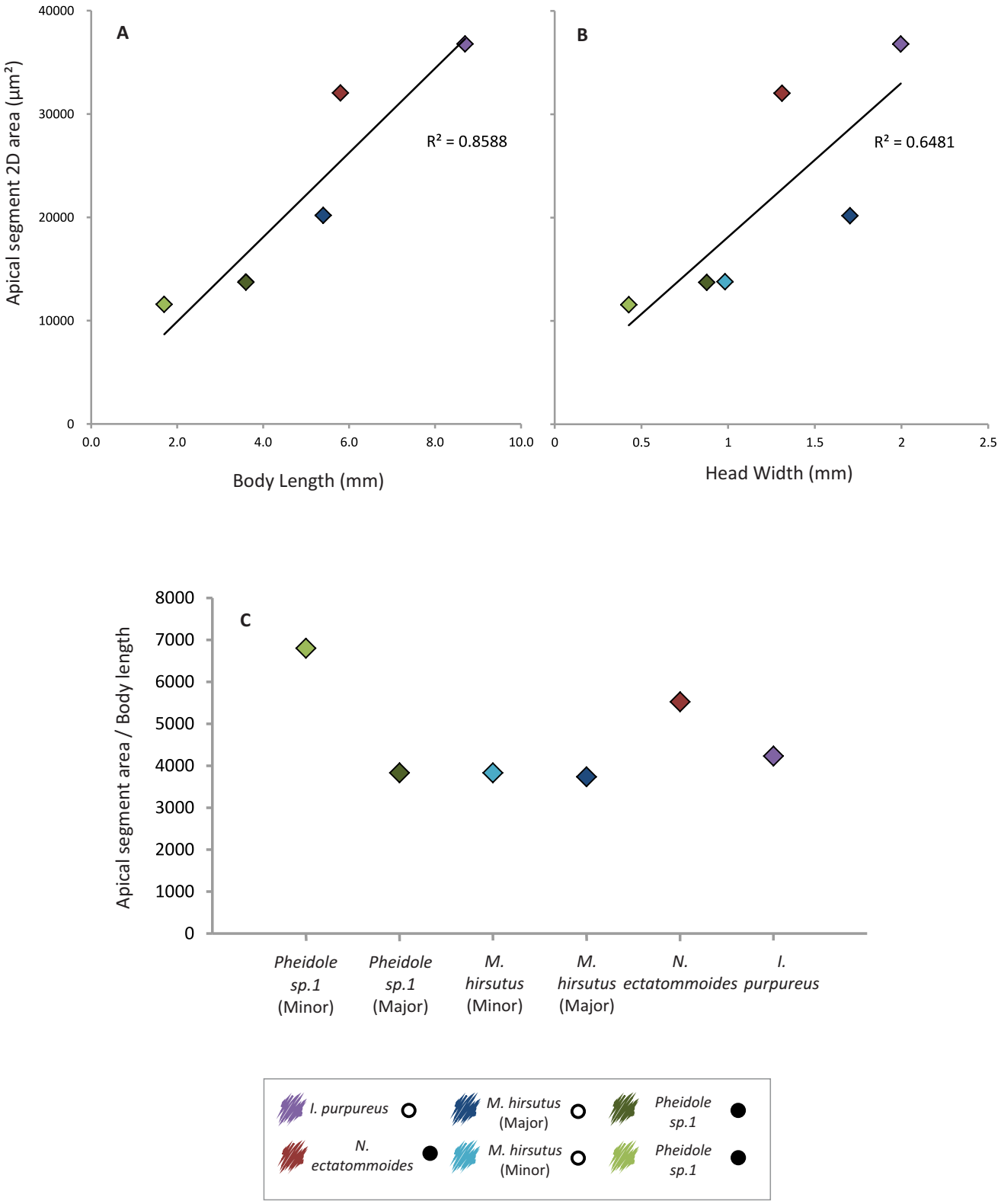

Figure 9

Relation of apical segment area (in two-dimensions) with different measures of body size for all six animals. **(A)** Scaling of apical segment area with mean body length. **(B)** Scaling of apical segment area with head width **(C)** Apical segment area normalised to body length. Colour codes for each animal is indicated. Regression line is indicated by continuous black line. Day-active (open circles) and night-active (closed circles) ants are indicated.

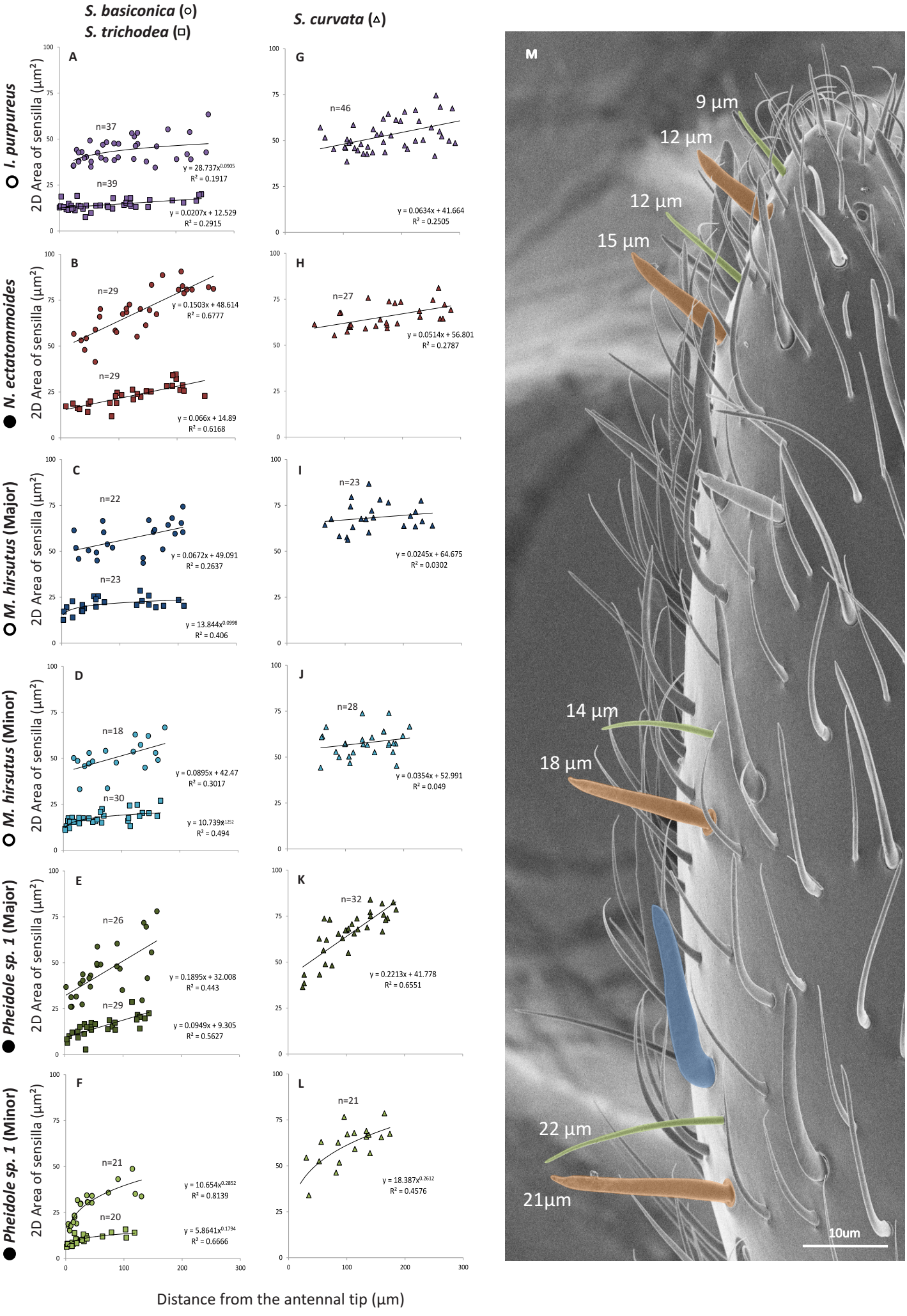
S. basiconica (○)
S. trichodea (□)
S. curvata (▵)
○ I. purpureus
● N. ectatommoides
○ M. hirsutus (Major)
○ M. hirsutus (Minor)
● Pheidole sp. 1 (Major)
● Pheidole sp. 1 (Minor)
2D Area of sensilla (µm²)
A
n=37
y = 28.737x^0.0905
R² = 0.1917
n=39
y = 0.0207x + 12.529
R² = 0.2915
G
n=46
y = 0.0634x + 41.664
R² = 0.2505
B
n=29
y = 0.1503x + 48.614
R² = 0.6777
n=29
y = 0.066x + 14.89
R² = 0.6168
H
n=27
y = 0.0514x + 56.801
R² = 0.2787
C
n=22
y = 0.0672x + 49.091
R² = 0.2637
n=23
y = 13.844x^0.0998
R² = 0.406
I
n=23
y = 0.0245x + 64.675
R² = 0.0302
D
n=18
y = 0.0895x + 42.47
R² = 0.3017
n=30
y = 10.739x^1252
R² = 0.494
J
n=28
y = 0.0354x + 52.991
R² = 0.049
E
n=26
y = 0.1895x + 32.008
R² = 0.443
n=29
y = 0.0949x + 9.305
R² = 0.5627
K
n=32
y = 0.2213x + 41.778
R² = 0.6551
F
n=21
y = 10.654x^0.2852
R² = 0.8139
n=20
y = 5.8641x^0.1794
R² = 0.6666
L
n=21
y = 18.387x^0.2612
R² = 0.4576
0
25
50
75
100
0
100
200
300
Distance from the antennal tip (µm)
M
9 µm
12 µm
12 µm
15 µm
14 µm
18 µm
22 µm
21µm
10um

Figure 10

Summary plate describing the change of size in chemoreceptive sensilla with distance from the tip increases. Plots **(A)** through to **(F)** show size variation in sensilla basiconica (circles) and sensilla trichodea (squares) in different species of ant (colour coded). Similarly plots **(G)** through to **(L)** describe the size variation in sensilla curvata (triangles). A total of five animals were surveyed for each species while the sample size (n) given within the plots represents the number of sensilla measured. The equation for each regression line and the R^2 value is given next to each line. The colourised SEM **(M)** gives an example of the size gradient of s. basiconica (orange) and s. trichodea (green) along the apical segment of the antenna of a *Pheidole sp. 1* minor worker. The length of each sensillum is given next to it in white. An example of s. curvata (blue) is also shown.

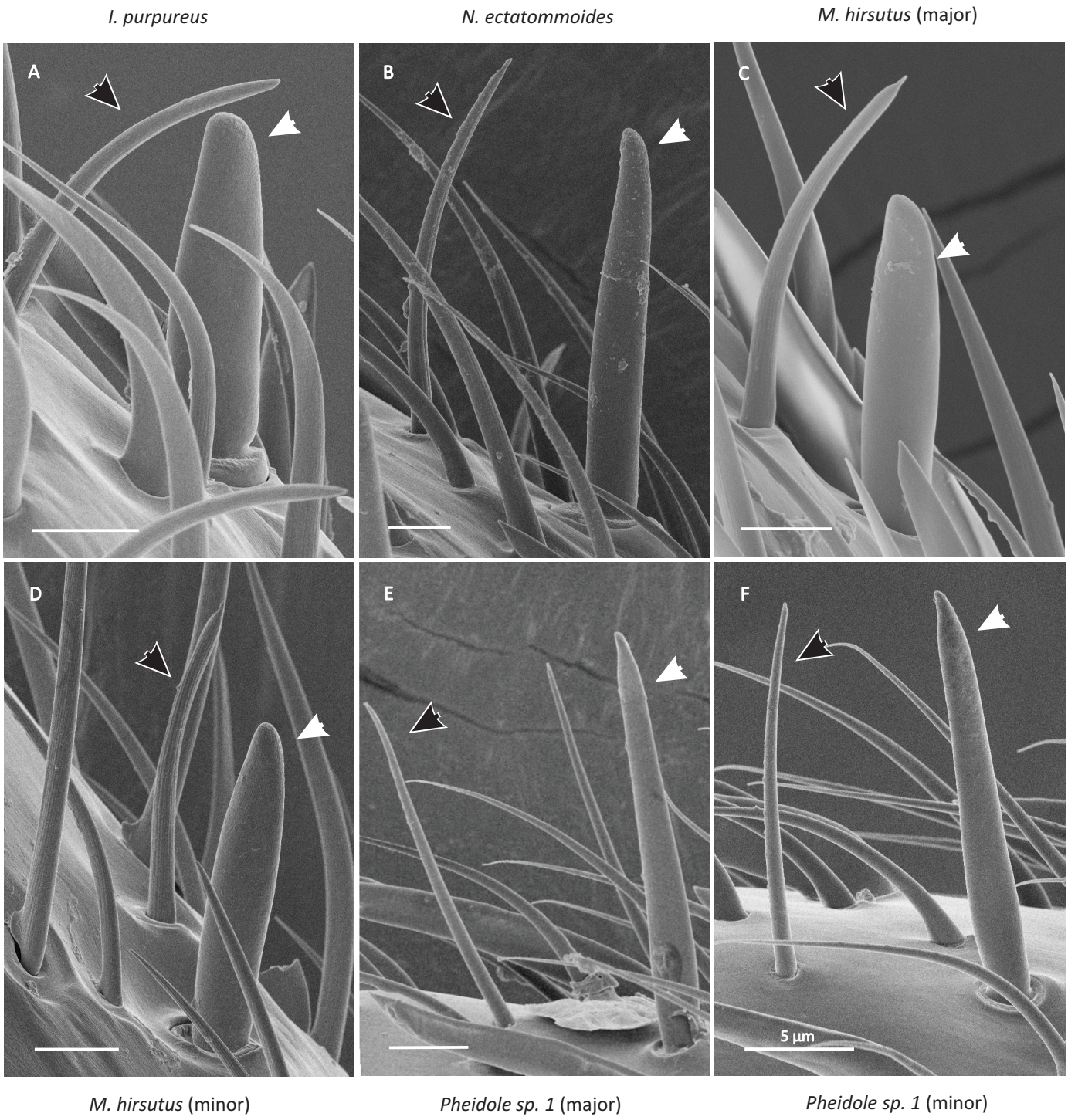

Figure 11

Typical examples of the thickened sensilla basiconica (white arrow) paired with the slender sensilla trichodea (black arrow). Panels **A-E** represent each of the six studied animals. All scale bars = 5µm.

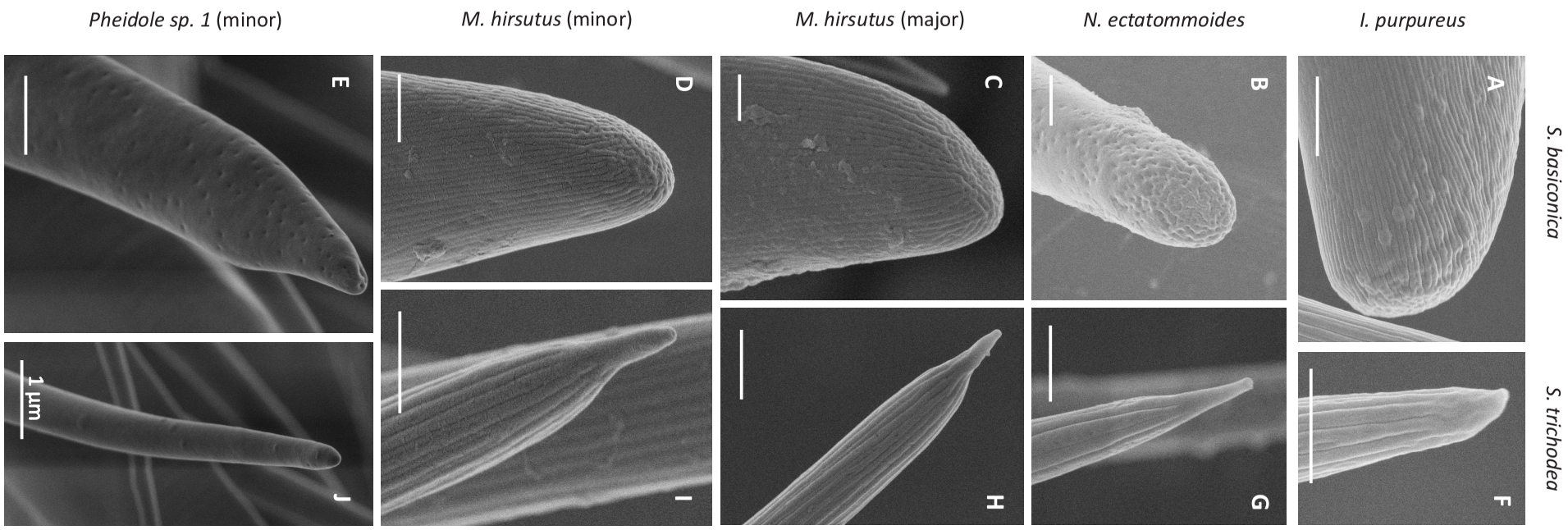

Figure 12

High magnification images of the tips of paired sensilla. **(A-E)** Sensilla basiconica and **(F-J)** sensilla trichodea showing the different patterns of striation and pores in five of the six studied animals. No images of *Pheidole sp. 1* major workers were available. All scale bars = 1µm.

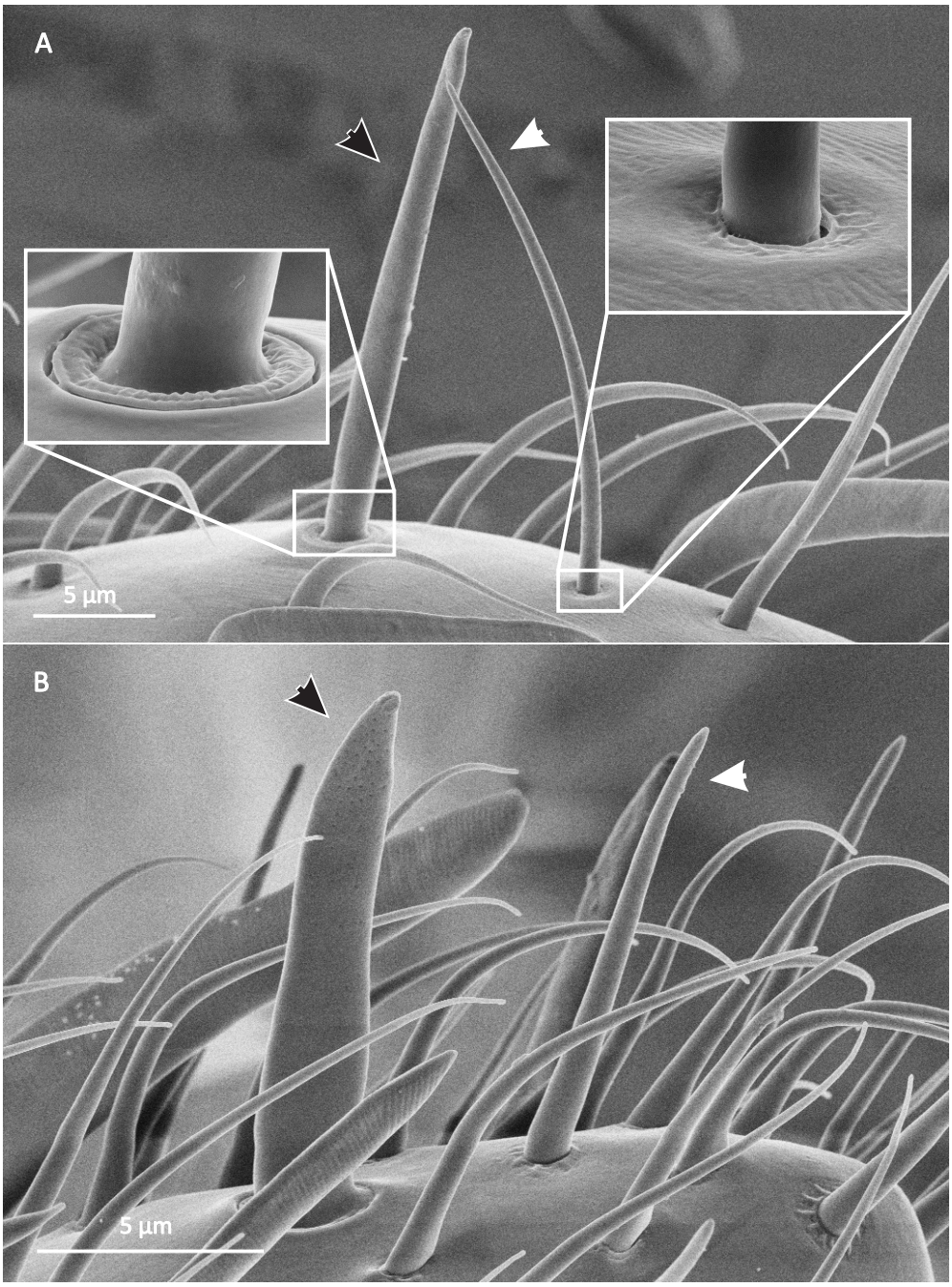

Figure 13

Morphological difference in the sensilla basiconica of *Pheidole sp. 1* minor worker. **(A)** An extremely long sensillum basiconicum (black arrow) found towards the base of the antennal segment, and **(B)** an extremely small sensillum basiconicum (black arrow) found very close to the tip. Insets illustrate details of the base of sensilla. Paired sensilla trichodea are also shown (white arrows). Note the variation in the scale bar length. All scale bars = 5µm.

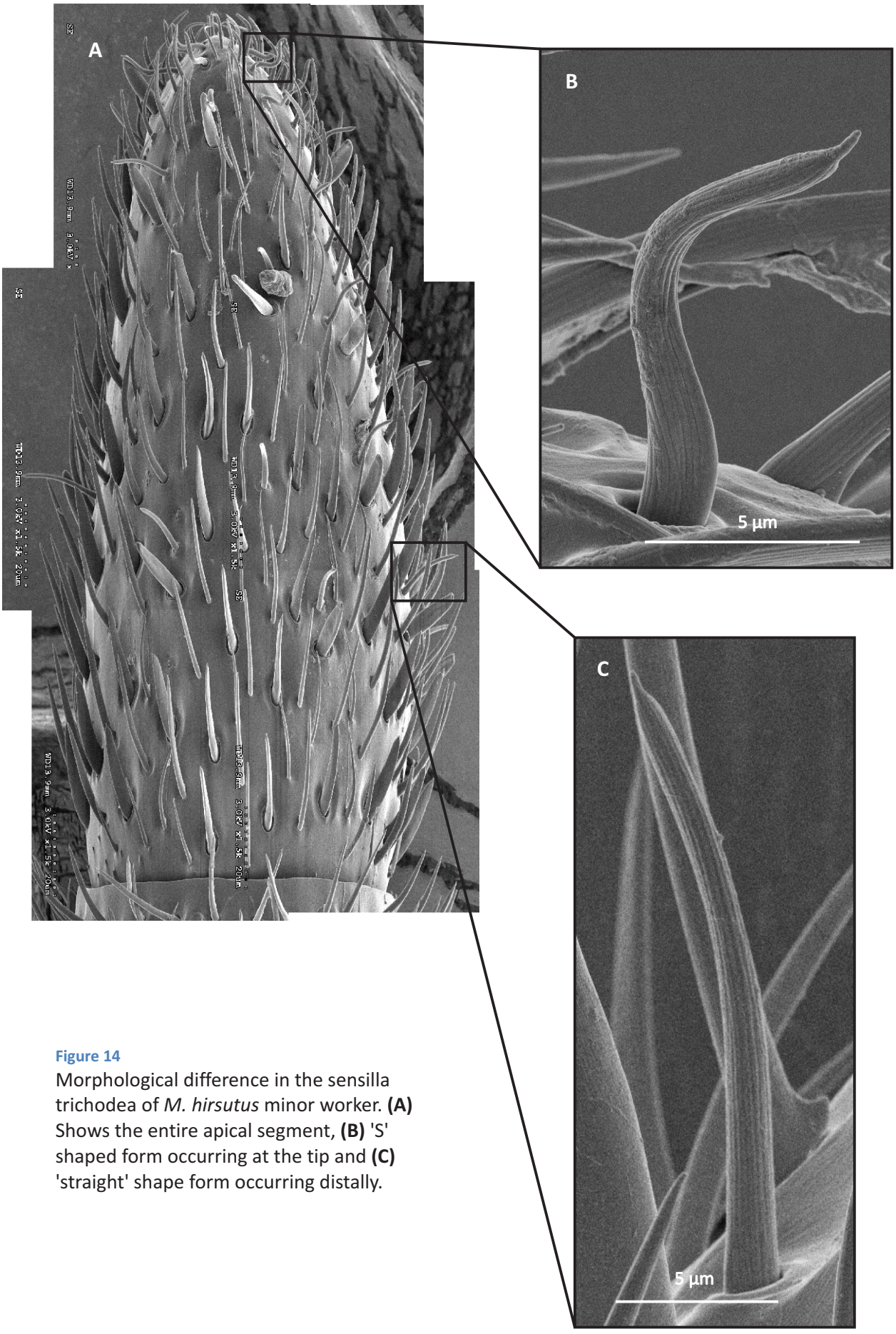

Figure 14

Morphological difference in the sensilla trichodea of *M. hirsutus* minor worker. **(A)** Shows the entire apical segment, **(B)** 'S' shaped form occurring at the tip and **(C)** 'straight' shape form occurring distally.

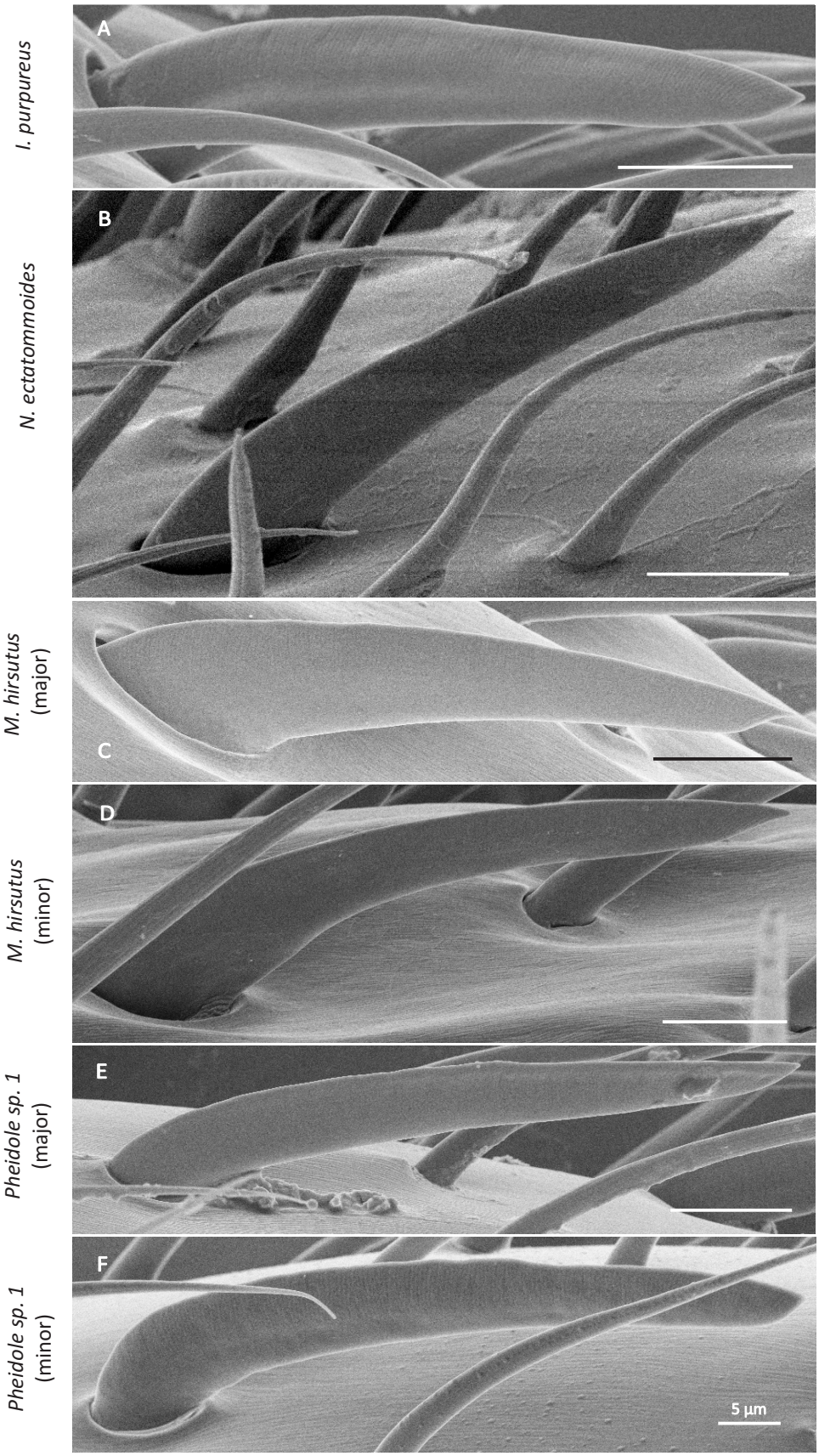

Figure 15

Typical examples of the sensilla curvata in different ants. Each panel **(A-F)** represents each of the six studied animals. All scale bars = 5µm.

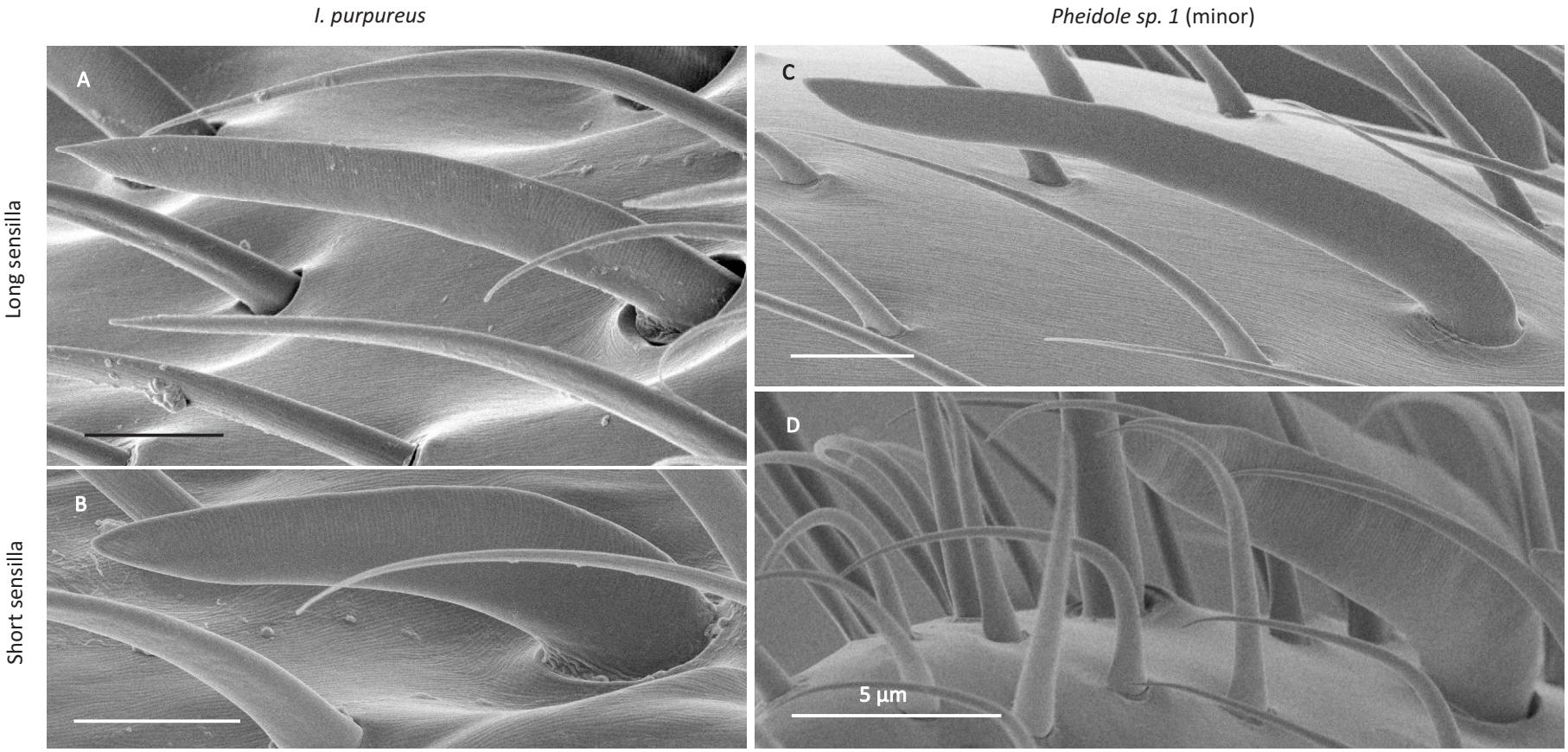

Figure 16

Differences in shape of the sensilla curvata within the largest studied ant, *I. purpureus* and within the smallest studied ant *Pheidole sp. 1* minor. Long sensillum of **(A)** *I. purpureus* and **(B)** *Pheidole sp. 1* minor, compared with short sensilla **(C,D)** of the respective species. All scale bars = 5µm.

Figure 17

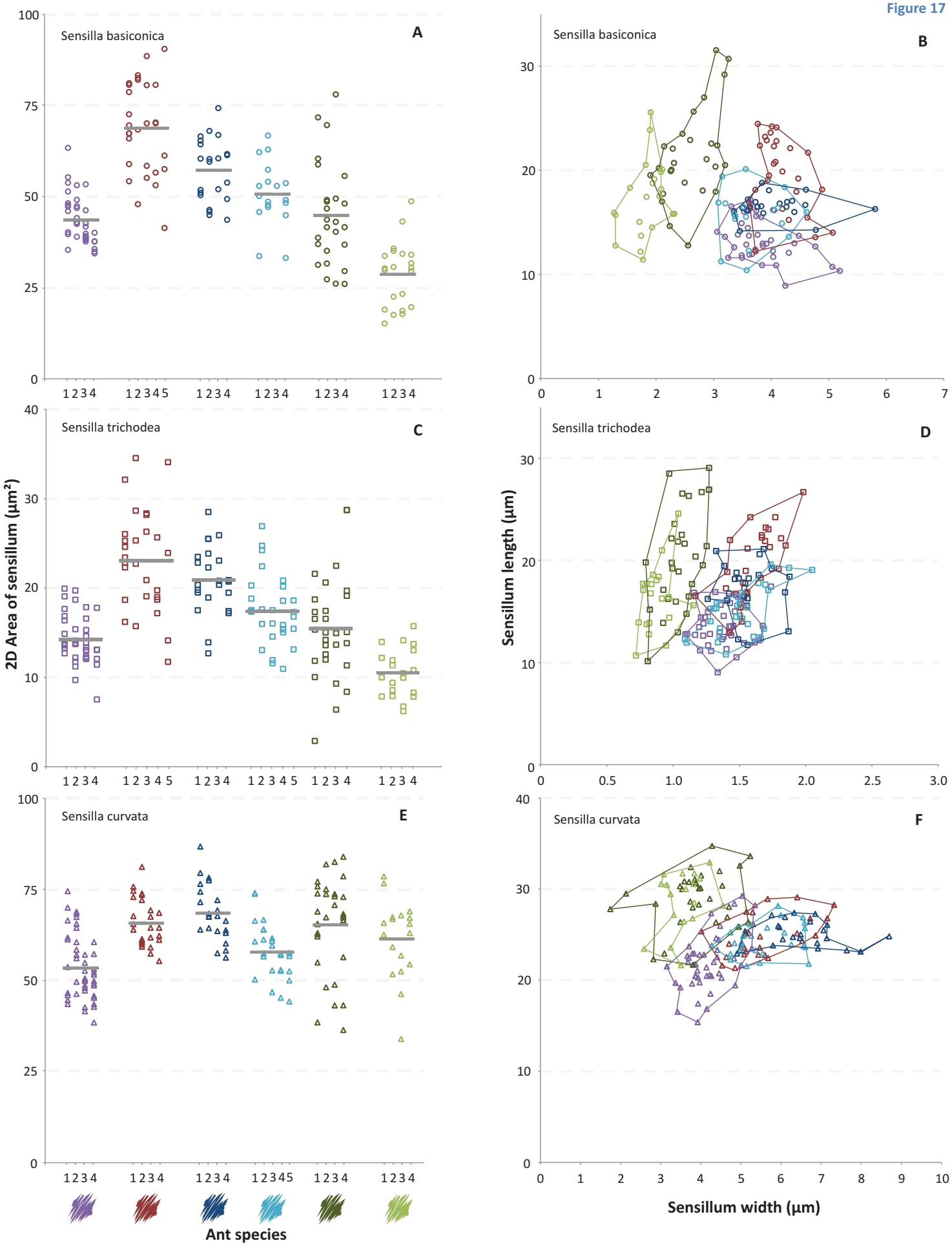
Sensilla basiconica
A
Sensilla basiconica
B
Sensilla trichodea
C
Sensilla trichodea
D
Sensilla curvata
E
Sensilla curvata
F
2D Area of sensillum (µm²)
Sensillum length (µm)
Sensillum width (µm)
Ant species
1 2 3 4
1 2 3 4 5
I. purpureus
M. hirsutus (Major)
Pheidole sp.1
N. ectatommoides
M. hirsutus (Minor)
Pheidole sp.1

Figure 17

Scatterplots summarising the intra- and interspecific variation in the dimensions of sensilla basiconica (circles), trichodea (squares) and curvata (triangles) in three species of ant (see colour code). Figures **A**, **C**, and **E** illustrate the range of sensillum sizes found on each individual measured (1-5 x-axis) with the species mean denoted by a solid grey bar. Figures **B**, **D** and **F** compare the distributions of width and length among different species.

3.4.1. Scaling: Size and numbers of sensilla relative to species size

Number of sensilla

Larger ants had a greater absolute abundance of all three sensilla (Figure 5 A). The first measure of size used to study the way in which the number of sensilla scaled with the size of an ant was head width. This seemed appropriate as ants bear these sensory structures and their accompanying nervous innervation, trachea, etc. on the antennae which are directly attached to the head. However, scaling the number of sensilla to head width did not result in a particularly strong correlation (see Figure 7 B, E, H). To further investigate this surprising result, body length was substituted for head width. This resulted in a stronger correlation (see Figure 7 A, D, G) but still did not seem like an appropriate explanatory variable.

The variable most directly influencing the number of sensilla an antenna can accommodate is the space available. Surface area limits the amount of space available for the outer cuticular element of sensilla, while volume limits the number of neurons and tracheae, as well as haemolymph flow (Schneider, 1964). Given the difficulty of obtaining volumetric measurements of the apical segment of the antenna, surface area was calculated instead. From this a strong correlation between the number of sensilla and the apical segment area was observed (see Figure 7 C, F, I). Furthermore, it appears that night-active species, with the exception of *Pheidole sp. 1* major workers, have larger apical segments relative to body size (Figure 9 C). This may be an adaptation to increase the number of sensilla. *N. ectatommoides* and *Pheidole sp. 1* minor workers do seem to have slightly more sensilla than would be expected for their size (Figure 7).

The only exception to the trend of increasing numbers with increasing body size was *Pheidole sp. 1* major workers. Here the number of sensilla, particularly sensilla curvata, were noticeably lower than in the similarly sized *M. hirsutus* minor. However, *Pheidole sp. 1* major workers seem to compensate for this, at least to some degree, by increasing sensillum size (see Figure 7). Alternatively, differences in task allocation may mean that major workers which act as soldier ants do not require as elaborate a sense of smell as their smaller, foraging counterparts.

There was no observable difference in chemoreceptor abundance relative to time of day active.

Size of sensilla

There were no major differences observed in trends arising from scaling with different measures of size such as body length, head width and apical segment area (compare across columns in Figure 8). Furthermore, because of the large variation in the size of sensilla within each species, it seemed inappropriate to compare means or to attempt any sort of regression. For this reason only obvious trends will be discussed.

Sensilla basiconica and trichodea tended to increase in size (i.e. area) with increasing body length, head width and apical segment area but this did not hold true for sensilla curvata (see Figure 8). The trends observed in the first two sensilla are very similar and shall be discussed first as their paired organisation might mean that they are under similar selective pressures. *Pheidole sp. 1* minors had

the smallest sensillum areas, while *N. ectatommoides* had the largest (Figure 8 A, D). *I. purpureus* did not follow this trend: instead, much smaller sensillum areas were observed in this species, comparable to those of *M. hirsutus* minors. This occurred in spite of the large difference in body sizes (*I. purpureus* BL = 8.7mm, *M. hirsutus* minor BL = 3.6mm). Shorter sensilla may be less prone to breakage, potentially driving animals with large numbers of sensilla to reduce their size. However, this seems unlikely in this case as *N. ectatommoides* has a similar absolute number of sensilla to *I. purpureus* (Figure 5 A) and yet the former species possesses the largest sensilla in this study. This dramatic reduction in size seems very peculiar but there appears to be no obvious explanation from the data collected here. It is possible that other factors of this species' ecology, such as foraging behaviours, may explain this reduction in sensillum size.

The size of sensilla curvata was remarkably consistent across all species (Figure 8 G, H, I). This could indicate that for some reason the design of this sensillum is such that it does not permit a great deal of variation. However, this seems unlikely given that curvata display a large amount of variation even within a single species (maximum range is approximately 50µm²). Further studies which take into account internal anatomy, may reveal more information about this sensillum which may explain this peculiar consistency across species.

3.4.2. Relative abundance of different types of sensillum and previous studies

In addition to studying the effects of miniaturisation and day/night activity on chemoreceptors, this study provided the opportunity to compare the chemosensory array of various species in detail. Although previous studies have looked at the number of sensilla found per antennal segment in various species of ants, no study has compared the abundance and distribution of sensilla across several species. Results from a survey of the sensory sensilla of *Lasius fuliginosus* (Dumpert, 1972b) revealed similar trends to those observed in the species studied here. Sensilla curvata were the most abundant, followed by sensilla trichodea and sensilla basiconica. Another study of the sensilla of *Camponotus japonicus* (Nakanishi et al., 2009) found similar trends, but the abundances of sensilla basiconica and trichodea were indistinguishable. The relative proportions that each type of sensillum contributed to the total number of chemoreceptors were comparable across all species. However, there was some variation between species which did not seem to be explained by size. It is much more likely that ecological factors such as foraging behaviours may influence the relative abundance of different types of sensilla. This may be of particular importance if chemoreception is involved in finding different food sources. If this is the case, it is possible that the chemical cues and chemoreceptors used to find different types of food sources may be different, for instance chemical cues to live prey such as other insects (e.g. insect pheromones, volatile) versus chemical cues to seeds (e.g. carbohydrates, non-volatile).

Results from a number of studies (Dumpert, 1972b, Nakanishi et al., 2009, Renthal et al., 2003) indicate that the largest proportion of chemosensory sensilla, or indeed of any type of sensilla, are found in the apical segment (Figure 18). Renthal *et al. (*2003) also found a high number of sensilla in the basal segment but they do not differentiate between different types of sensilla in their survey so this may be due to the high number of mechanoreceptors generally found in this segment (personal

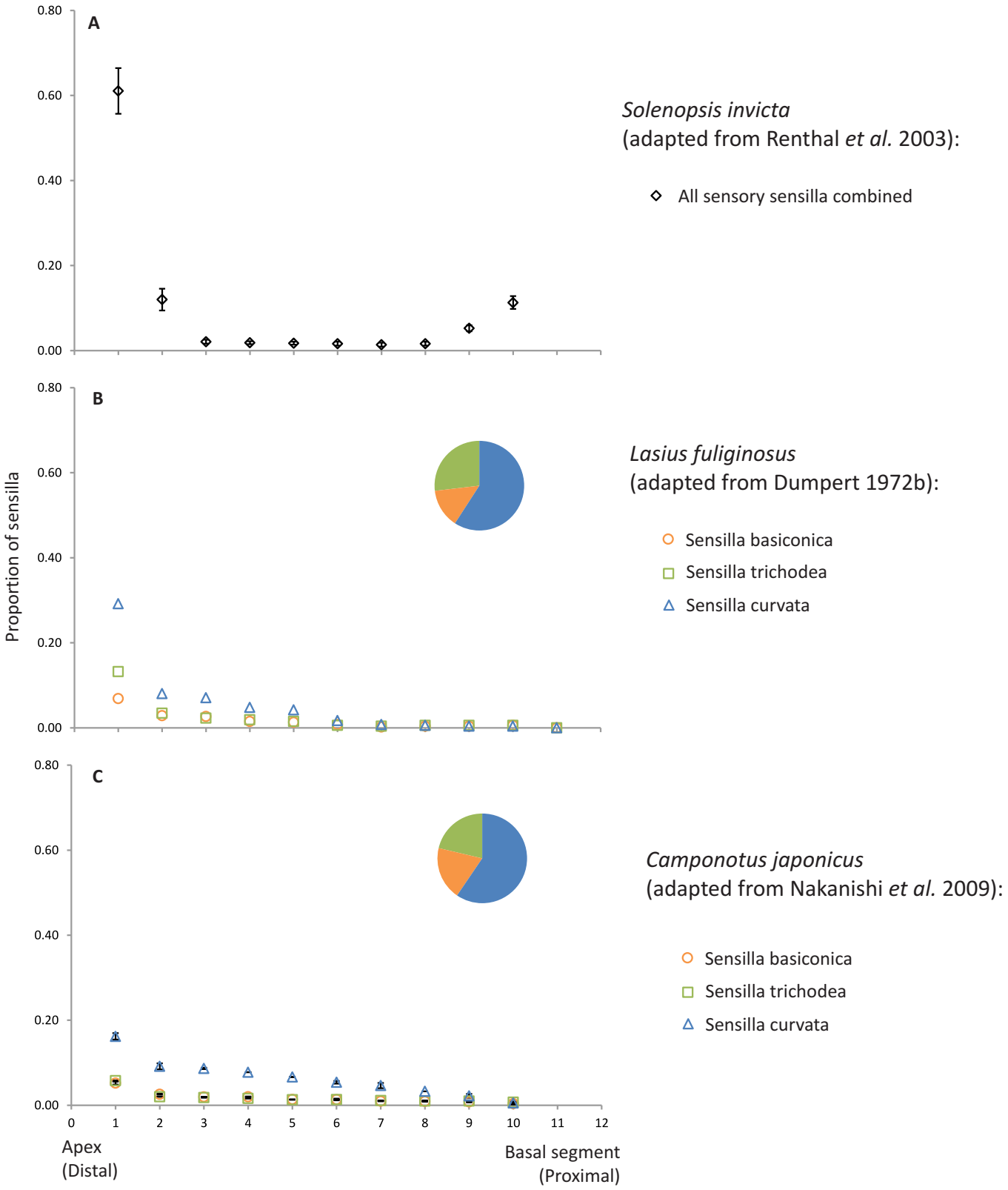

Figure 18

Abundance of sensilla in all antennal segments in three different ants. **(A)** All sensory sensilla of *Solenopsis invicta*. Adapted from Renthal et al. (2003) who included chemo- and mechanoreceptors, due to which the basal segment shows a peak in the abundance of sensilla (x̄±SE, n=10, total number of sensilla=858). **(B)** Proportion of the three sensilla from only one worker ant of *Lasius fuliginosus*. Adapted from Dumpert (1972b) (total number of sensilla=521); **(C)** Proportion of the three sensilla in worker ants of *Camponotus japonicus*. Adapted from Nakanichi et al. (2009) who used a different nomenclature (sensilla basiconica = basiconica, sensilla trichodea = chaetic-A, curvata = trichoid-I) but sensillum types were identified from the SEM (x̄±SE, n=2, total number of sensilla=1036). Data is normalised to the total number of sensilla reported by each study. Pie charts represent the proportion contributed by each chemoreceptor sensillum.

observation, FRE). Consequently, surveys of the apical segment only, instead of the whole antenna, should be strong predictors of the state of affairs throughout the antenna.

3.4.3. Notes on the general morphology of sensilla

There were a few peculiarities in the morphology of sensilla which could not necessarily be linked to size related functional adaptations. For instance the thickness of the cuticle making up the rings around the base of sensilla basiconica seemed to vary considerably between species. In *M. hirsutus*, for example, the sensillum appears to be attached to the thickened ring by a section of membranous cuticle, with the ring itself being relatively thin and flexible-looking (Figure 11 D). This was also the case in *N. ectatommoides* and the thinner sensilla in *Pheidole sp. 1* (see Figure 13 A, inset). However, in *I. purpureus* and in the thicker sensilla of *Pheidole sp. 1* the ring appeared to be stiffer and most probably fused to the shaft of the sensillum (see Figure 11 A and Figure 13 B). However, it was in the former only that the ring was considerably wider and elevated above the cuticular surface. Another, peculiarity observed in this species was the presence of small bumps around the pores which somewhat resembled the gustatory papillae of the human tongue (Figure 12 B). The basiconica insertions of *Pheidole sp. 1* (major and minor workers) differed between small and large sensilla. Longer sensilla may need a more flexible, articulated insertion to prevent breakage, while in the smaller sensilla the ring of cuticle is fused to the sensillum.

Although sensilla trichodea were generally straight or gently curved, in the medium sized *M. hirsutus* the sensilla in this apical area were often tightly twisted into 'S'- shapes (see Figure 14). This did not occur in any other species, although in the larger *I. purpureus* and *N. ectatommoides* the distal sensilla trichodea tended to be more strongly curved. This seems to be paradoxical as curved sensilla occupy more surface area. However, considering that there is a limit to how close together sensilla can be before the lack of space impedes the permeation of chemical signals through to the pores of sensilla, the presence of curved sensilla at the antennal tip may make sense (Koehl, 2001). The curves of sensilla trichodea may act to create more space between sensilla and assist fluid flow of air or chemical bearing substrates. Alternatively, and more simply, if the tip of the apical segment is used for contact chemoreception, sensilla may become bent from the constant pressure.

An interesting effect possibly related to the packing of sensilla was the size ordering which occurred in *N. ectatommoides* and *Pheidole sp. 1.* In these two species sensilla tended to decrease in size as they approached the apex of the antenna. It is likely that the reason size ordering is observed predominantly in *Pheidole sp. 1* and *N. ectatommoides* and not elsewhere is because these two species have longer than average sensilla. This could lead to difficulties in packing of sensilla at the crowded tip. A simple solution to this would be to decrease the size of the distal sensilla which is exactly what these species do. The question of why these species should have such long sensilla still remains. The two species are of very different sizes but they are both night-active. A higher reliance on chemical cues could select for longer sensilla with more pores to improve odour capture. The presence of additional pores, however, was not tested and so it is not possible to make such a conclusion. Additionally neither of these species exhibited striations on their sensilla basiconica, and *Pheidole sp. 1* (major and minor workers) had no striations on their sensilla trichodea either. If striations are indeed openings leading to chemosensitive dendrites then elongation of the sensilla

may be a way to compensate for the lack of striated openings, although this once more assumes that extra length leads to additional pores. The trend was generally strongest in sensilla basiconica and trichodea and weakest in sensilla curvata. This was probably because sensilla curvata generally did not occur near the apex (see Figure 10). The exception to this rule was *Pheidole sp. 1,* where sensilla curvata started just beyond the crown of sensilla trichodea, in this case the size ordering effect of sensilla curvata was comparable to that of the other sensilla. In conclusion, while there are reasons to believe that the size ordering effect should be stronger in *N. ectatommoides* and *Pheidole sp. 1,* it is probable that a similar effect occurs at a smaller scale in the other species. While the R^2 values of the other plotted sensilla often fail to indicate a strong relationship it must be pointed out that the relationships are often destroyed by the large amount of size variation found in the proximal part of the apical segment. Small datasets may also be a contributing factor in certain cases (especially in the case of the curvata of *Pheidole sp. 1* minors).

Research by Dumpert (1972b) indicates that sensilla curvata are sensitive to alarm pheromones of various kinds. This function as a chemoreceptor of volatiles is consistent with the observed distribution of the sensilla away from the tip of the antenna in the studied species. Renthal et al. (2003) describe the antennation behaviour of *Solennopsis invicta* and identify the tip and surrounding dorsal area as the main contact surfaces. It may be interesting to compare the abundance of sensilla curvata on the dorsal and ventral surfaces of the apical segment. It may also be useful to identify contact surfaces by providing live ants with a coloured, finely ground food substrate which could stick to the antennae upon contact.

Further studies

Questions regarding the internal morphology of sensilla remain open but more time intensive analysis with techniques such as silver nitrate staining (Dumpert, 1972b, Renthal et al., 2003) and sectioning of sensilla for TEM is necessary to address these questions. One important issue that needs to be addressed is whether the external openings observed actually lead to dendritic segments. Of particular interest is whether both striations and pores observed in sensilla basiconica of certain species lead to dendritic segments. The number of neurons innervating each sensillum should also give an indication of the resolving capability of individual sensilla and it would be interesting to establish whether or not there is variation in the internal morphology of externally indistinguishable sensilla. Another unresolved issue was whether or not sensilla trichodea are pore-bearing sensilla. The presence of openings on sensilla trichodea could not be confidently established due to the extremely small size of putative pores. Slits and striations observed in some species may represent openings leading into the lumen but staining with silver nitrate is necessary to answer this question. Also important is the antennal volume available to house the relevant nerves, trachea and haemolymph (Schneider, 1964). Finally, this study has only covered morphological variation and organisation, with some speculation on function, but in order to confidently establish the function of sensilla, behavioural and electrophysiological studies are absolutely necessary.

Although a novel Bauplan was not observed here this may be because the smallest ant studied *Pheidole sp. 1*, although extremely small (1.7mm long) is not yet at the limit of ant miniaturisation. Some species from the genus *Carebara* may be under 1mm in length. However, these ants do not occur in Australia. Furthermore, the problems encountered working with *Pheidole sp. 1* are only

likely to be compounded in even smaller ants. Therefore, it is important to develop specialised protocols for the processing of small animals before embarking on a more in depth study of small species of ant.

4. Compound eyes

4.1. Introduction

As central place foragers ants use two main strategies for navigating to a food source and back to the nest, both of which largely depend on the use of visual cues. These strategies consist of path integration and landmark guidance. For path integration, an ant leaving the nest will constantly update its vector information and use this information to determine the most direct route back to the nest (Collett and Collett, 2000, Wehner and Srinivasan, 2003). This is done by first storing information on heading direction relative to the nest by using a visually perceived celestial compass (Collett and Collett, 2000, Wehner and Srinivasan, 2003) and by determining the distance travelled by some form of step counting (Wittlinger et al., 2007). This information is then integrated by a homebound ant to compute the home vector. Similarly, landmark guidance heavily depends on vision as it requires outbound animals to memorise the location of specific landmarks and their appearance at various angles and distances from the nest (Kohler and Wehner, 2005, Narendra, 2007, Wehner et al., 1996, Zeil, 2012). As an animal returns it must match the previously stored views to the view currently being experienced.

Insect vision is a relatively well studied field and much is known about the structures and mechanisms involved especially, in hymenopterans. The structures responsible for vision in ants are two dorso-laterally positioned apposition-type compound eyes. These are composed of numerous self-contained, photosensitive units called ommatidia (for a detailed description of the eyes of the desert ant *Cataglyphis* see Brunnert and Wehner, 1973). Each ommatidium has a lens and a crystalline cone which together focus and channel light into the photoreceptive unit below called the rhabdom (Warrant and Nilsson, 2006). Each ommatidium is surrounded by screening pigments which prevent light channelled into one ommatidium from reaching adjacent ommatidia. Some ant species also possess ocelli, simple eyes located atop the head which have been implicated with the perception of the plane of polarised light (Schwarz et al., 2011); however, these will not be studied here.

Different aspects of an eye are known to influence the quality of visual input an animal can derive from it. For instance, it is known that visual sensitivity is dependent on the size of facets (i.e. lens diameter), rhabdom diameter, rhabdom length and overall size of the eye (Warrant and Nilsson, 2006). Increasing the diameter of optic structures maximises the probability that a photon will enter a given ommatidium while increasing the length of the rhabdom increases the probability that a photon will be absorbed by increasing the amount of photosensitive tissue a photon must travel through. Resolution, on the other hand, is largely based on the number of facets (or contributing 'pixels') which an eye possesses (Warrant and Nilsson, 2006). Given that the amount of space an animal can allocate to an eye is finite, these two factors, the size and the number of visual units, will compete with one another. This represents a major trade-off that animals must contend with which has been studied by comparing day- and night-active animals (Menzi, 1987, Moser et al., 2004, Warrant and Dacke, 2011, Greiner et al., 2007, Narendra et al., 2011). What has become apparent from these studies is that night-active animals sacrifice resolution for sensitivity and thus have fewer but larger optic units relative to day-active animals. Meanwhile day-active animals do the inverse:

since available light is not limiting in a day-active animal, optics can be made smaller to increase their number and therefore improve resolution.

It is clear that there is a strong understanding of how insect eyes work and how they change under a variety of circumstances. Eye adaptations have been studied not just for animals operating under different light conditions but also in the context of sexual dimorphism (Zeil, 1983), and in the case of eusocial species, caste differences have also been examined (Ribi et al., 1989, Baker and Ma, 2006, Klotz et al., 1992). This has given much insight into how functional requirements shape eye design, but these have not been studied in the context of miniaturisation.

The vision component of this study proposes to use previous knowledge of the physical limits affecting eye design to study the visual systems of different ant species operating at different size scales and under different light conditions. A study of large, closely related ant species of the genus *Myrmecia* (BL = 12.0 – 30.0 mm, HW = 3.8 – 4.0 mm) found significant changes to eye design accompanying changes in body size and time of activity (Narendra et al., 2011). However, *Myrmecia* is a phylogenetically basal group which has retained many ancestral traits including a potent sting, large mandibles and large eyes (Ward and Brady, 2003). This study examines whether changes to eye design are consistent across smaller, phylogenetically diverse ant species spanning a considerable size range (BL = 1.7 – 8.7 mm, HW = 0.4 – 2.0 mm).

4.2. Methods

4.2.1. Facet numbers, size and distribution

Eye facets were studied using a combination of eye replicas and SEM images. The typical number of facets seen in each species was determined based on SEM images showing the entire eye of five specimens of each species (left-right randomised). If the workers were polymorphic, five majors and five minors were sampled. Samples were coated with Au/Pd (20mA, 4 mins) and viewed using a Hitachi S-4300 SE/N FESEM (5kV, Aperture 4 (smallest), working distance ≈ 12.0mm). To obtain replicas of the cornea a method used by Ribi *et. al.* (1989) and Narendra *et al.* (2011) was employed. Transparent nail polish was used to paint the surface of the eye. Once dry, the nail polish was carefully peeled back and laid out on a glass microscope slide and flattened by placing a cover slip over it. The specimen number, left or right eye and orientation of the eye were recorded. If the replica was too curved to be flattened, small incisions were made using a scalpel. These 2D representations of the cornea were photographed using a Leica Upright DM6000 microscope mounted with a camera and mapped using a custom written, Matlab based program (Richard Peters, La Trobe University). This provided detailed information about the number, size and distribution of facets in a single individual of each species including major and minor workers. Eye area from four workers of each species and caste were also measured from these replicas.

Average facet diameters were obtained from measurements taken using ImageJ 1.45s (Rusband) in five individuals of each species and caste (10 randomly chosen facets per individual). These data were also later used to calculate the optical cut-off frequencies (υ_{co}) given by the formula: $\upsilon_{co}=A/\lambda$, where A=facet diameter (largest observed facet) and λ=wavelength (0.5µm for blue-green light). This defines the finest frequency spatial pattern transmitted by a lens which is able to be resolved (Land, 1997); in other words, it defines the resolving power of an eye with facets of a given size.

A simulation was carried out which approximated the amount of spatial detail available to an animal with a given number of ommatidia. This was done by estimating the interommatidial angles from the number of facets in an eye under the assumption that the visual field of an eye extended over a hemisphere:

20626° / number of facets = interommatidial angle

Where 20626 is number of degrees subtended by a hemisphere (area of a sphere = 12.56637 steradians, one steradian = (180/Pi)^2 square degrees).

Panoramic images of a natural scene were then filtered with the Gaussian blur function of CorelDRAW® Graphics Suite X5 (2010 Corel) to simulate the interommatidial angles calculated. This was done using a panoramic photograph covering 360 degrees in the horizontal direction and approximately 55 degrees in the vertical direction (courtesy of Jochen Zeil). By dividing the width of the photograph (2161 pixels) by the number of degrees imaged in the photograph (360 degrees) the number of pixels per degree was obtained (6 pixels/degree). This number was then multiplied by the calculated average interommatidial angle of the simulated eye and entered as the sigma value of the Gaussian blur function.

4.2.2 Internal anatomy

To study the internal anatomy of the compound eyes, specimens were sectioned for light and transmission electron microscopy. Three incisions were quickly made on the heads of live specimens to allow infiltration of fixative before the onset of tissue decay and to assist resin infiltration later on. The incisions removed the mouth parts and the posterior and ventral portions of the head. Immediately after the incisions were made the tissues were placed in specimen vials filled with aldehyde fixative (4% paraformaldehyde and 2.5% glutaraldehyde, Electron Microscopy Sciences) and left on a shaker table for four hours. The samples were then washed with distilled water (two washes), placed in 2% osmium tetroxide solution (Electron Microscopy Sciences) to stain lipid tissues and left on the shaker table for one hour. Each subsequent treatment made use of the shaker table to assist mixing and infiltration into the tissues. Samples were washed a further two times with distilled water and taken through an ethanol dehydration series (50, 70, 80, 95% for 10 minutes each and then two treatments of 100% for 15 minutes each). After dehydration, samples were treated twice with propylene oxide (ProSciTech; 20 minutes per treatment) to assist with infiltration of the resin used later on.

Infiltration was carried out by taking samples through propylene oxide/Epoxy resin mixtures (FLUKA) with increasing concentrations of resin. The series used was as follows:

- 2:1 for 3 hours
- 1:1 overnight
- 1:2 for 4 hours
- Pure resin overnight

The samples were transferred to new vials at each step and left on a shaker table for the duration of each treatment. The last step was carried out with the vials uncovered to allow evaporation of any residual propylene oxide.

The samples were mounted on the small face of pre-prepared resin blocks. This made the orientation of the eyes easy to observe through the thin layer of resin coating the sample. Once mounting was completed the samples were placed in an oven at 65°C for 12 hours. When polymerisation was complete the heads were split in two using a small hacksaw and razor blades and re-mounted. This permitted positioning of the eyes in such a way that they were directly facing the microtome knife, thus providing perfect cross-sections of the medial rhabdoms. Re-mounting was done by either attaching the sample with some of the surrounding resin to the small face of a block using a drop of fresh resin or by stripping back the old layer of resin from the sample and re-embedding it inside a drop of fresh resin placed on the new block. All remounted samples had to be placed in the oven for a further 12 hours before they could be used for sectioning.

Light and EM sectioning was carried out on a Leica EM UC7 ultramicrotome. For light microscopy, glass knives were used to collect 2µm thick sections. Samples were mounted onto glass slides, heat fixed (~15 minutes) and stained using toluidine blue (Sigma). Images were obtained using a Leica Upright DM6000 microscope mounted with a Spot Flex Color FX1520 camera (Diag Inst, MI, USA). For EM sectioning a Diatome ultra 45° diamond knife (size 2.5) was used to obtain 75nm thin sections which were collected onto coated single slot copper grids (ProSciTech, slot 1000x2000).

Grids were coated using the following method. Unfrosted glass slides were cleaned using ethanol and allowed to air dry, then slowly dipped in 2% formvar solution. Slides were then propped against a vertical surface so that they were as vertical as possible and allowed to dry for two minutes. Using a razor blade, four incisions were made on the coating which outlined a rectangle in the middle of the slide. The first slide to be used was then 'breathed on' to dampen it and slowly dipped into a clean shallow bowl filled with milli-Q distilled water up to the rim. The slide was then slowly pulled out leaving a rectangular section of formvar coating floating on the surface of the water. Pre-cleaned (sonicated in acetone) copper slot grids (slot 1000x2000) were then gently dropped onto the floating formvar using forceps and keeping the shiny surface of the grids facing upwards. Once covered with grids, the formvar was lifted off the surface of the water using a rectangular piece of nescofilm. The nescofilm was cut to be two or three times the size of the floating formvar and slowly lowered on top of it until the nescofilm was floating on the surface of the water. The nescofilm was then gently lifted by one corner so that the formvar adhered to it and then placed on a petri dish lined with filter paper with the grids facing upwards. The grids were then allowed to dry overnight before being used.

Once EM sections were collected onto the coated grids the samples were stained using 2% uranyl acetate (UA) and Reynold's lead citrate (1.6% lead citrate mixed from Electron Microscopy Science supplies). Small droplets of UA were placed onto a piece of nescofilm then each grid was placed on top of a droplet, sample side down. The grids were protected using a petri dish covered with aluminium foil to block out light and left for 10 minutes. The grids were then washed by dipping into two separate beakers filled with distilled water, and then excess water was removed by gently dabbing the side of the grid against a piece of filter paper. Sodium hydroxide pellets were arranged on a new piece of nescofilm and droplets of lead citrate were placed next to these pellets. It is necessary to use sodium hydroxide pellets and avoid breathing on the lead citrate droplets as this stain is extremely sensitive to moisture and will form crystals. Each grid was once more placed onto a droplet, sample side down, covered by the petri dish and left for a further 10 minutes. At the end of this time the grids were picked up using forceps, ensuring the formvar coating did not rip, and

dipped in beakers of distilled water to wash excess stain off. The grids were then dabbed on filter paper, placed on a grid holder and left to dry overnight before being observed under the transmission electron microscope (TEM).

Images were captured using a Hitachi HA7100 TEM (accelerating voltage of 75kV; aperture 3 (medium); spot size 3 (medium)) fitted with an Orius 832.H04WO camera (Gatan Inc., USA). The eucentric height was set for each sample imaged. Only rhabdoms located in the central portion of the eye were imaged as these were perpendicular to the sectioning plane whereas peripheral rhabdoms did not and therefore were not perfect cross-sections.

4.3. Results

4.3.1. External anatomy: Eye area, Number of facets and Facet size

Eye area showed a strong positive correlation with body length (Figure 19 A, B). The largest measured eye area was 122,330 μm² (*I. purpureus*) and the smallest was 6,722 μm² (*Pheidole sp. 1* minor). Despite this tight correlation between eye area and body length, *Pheidole sp. 1* major workers exhibited an eye area well below what would be expected for an ant of such dimensions. These ants had eyes approximately a quarter of the size of the eyes of *M. hirsutus* minor workers despite the fact that both of these animals had practically identical body lengths.

Cornea replicas were used to generate facet maps which graphically illustrated the changes in facet area across different species (Figure 20 A, B). Quantitative data was also obtained which showed that the number of facets increased with body size (Figure 20 A, C). The largest species, *I. purpureus,* was found to have an average of 496 facets while the smallest species, *Pheidole sp. 1* minors, had an average of 21 facets. However, body size was not the only factor affecting the number of facets. Time of activity played a role as well, with the night-active animals having fewer facets than day-active ones. This was particularly apparent in *N. ectatommoides.*

The nocturnal species *N. ectatommoides* and *Pheidole sp. 1* (majors and minors) had much larger facets relative to day-active species (Figure 20 A, D). This was less noticeable in the minor workers of *Pheidole sp. 1* which predominantly had medium sized facets (green) rather than the extremely large (red) facets observed in their larger counterparts. *Pheidole sp. 1* (majors and minors) was also peculiar in the relative frequency distribution of facet areas (Figure 20 B). While other species had facet areas which approximated a normal distribution, this species exhibited an erratic, discontinuous pattern of distribution with some extremely large and some extremely small facets. This can be, at least partially, attributed to the low number of facets present in their visual array. Furthermore, facet maps were obtained from a single individual of each species, and while providing a useful representation of the whole visual array, must be treated with care as it does not capture any variability which may exist within each species.

To obtain a more representative, quantitative depiction of the variation among individuals in the external visual array across species, cornea replicas and SEM images from different individuals of the same species and caste were studied (n=2-5 depending on species and caste: see Figure 20). Figure

20 C and Figure 20 D illustrate the variation in facet numbers and diameters not only between species but also within each species and caste. Once more the night-active species stand out from their day-active counterparts. This is particularly evident in *N. ectatommoides.* Night-active species tend to have fewer yet larger facets. Additionally, very little variation between individuals of the same species and caste is observed in both facet numbers and diameters.

Results from optical cut-off frequency calculations indicated that animals active at the same time of the day had similar cut-off frequencies (Figure 24 A). According to these calculations, day-active animals have a better resolving power than night-active animals. Similar trends are seen when examining the results from the Gaussian blur simulations (Figure 24 B). Day-active species have access to a larger quantity of spatial information due to the greater number of facets while night-active species have fewer facets and access to less visual information. Here, however, *N. ectatommoides* stands out among the night-active species due to the larger number of facets which, despite their limited resolution, provide more 'pixels' and therefore more spatial information.

4.3.2. Internal anatomy: Rhabdom diameters

Images of the distal rhabdoms were obtained using light and transmission electron microscopy (TEM) (Figure 21 A, B). Light microscopy sections gave an overview of the layout of the eye which permitted identification of the distal rhabdoms as soon as they emerged in sections. TEM sections were collected at this point and used to obtain rhabdom diameter measurements (Figure 21C). Similar to the previously discussed trends in facet diameter, the night-active *N. ectatommoides* was clearly distinct from its day-active counterparts with rhabdom diameters over four times larger than the similarly sized (BL and HW) *M. hirsutus* major.

Unfortunately data for *Pheidole sp. 1* is not yet available. Processing such small animals (HW=0.43mm) incurred a number of unexpected challenges which are yet to be resolved. Fixation of tissues was problematic due to the difficulty of handling such small animals to create incisions in the head capsule. Additionally, the thin flexible cuticle resisted cutting with razor blades, crumpling and bending under the slightest pressure and damaging tissues in the process. Later processing also posed issues as the minute eyes were very difficult to orient correctly for cross-sectioning of the rhabdoms as they were difficult to see. The haphazard organisation of the few facets that were present also exacerbated the problem of orientation. This was because each facet faced a very different direction to all its neighbours meaning that at best only one facet could be sectioned transversely per eye. The minute size of the eyes also meant that semi-thin sections contained a very small proportion of resin and did not adhere to slides well (retention ≈ 1 in 10). This issue was mostly solved by employing adhesive slides (Apex Superior Adhesive Slides, Leica) which greatly improved retention rates. Finally, the small size of the eye meant that very little tissue was available; from longitudinal sections it seems that the rhabdom is only about 10µm long.

From the sections that were obtained for *Pheidole sp. 1,* a few observations may be made (see Figure 22). The lenses in these species are markedly biconvex, and quite thick (approximately 20µm). The crystalline cone appears to be remarkably small relative to the lens (approx. 8.6 µm), although it is not possible to say with great certainty whether any of the studied sections are perfect

longitudinal sections. Microvilli were observed in TEM images but these were organised in a curious 'S' shaped pattern, unlike the elongated rectangles which would be expected in longitudinal sections of the rhabdom or the round or polygon-shaped rhabdoms seen in cross-section. This 'S' shaped pattern cannot be explained by a skewed sectioning plane (Figure 22 B, *Pheidole sp. 1* major). Rhabdom-like structures were seen in light sections (Figure 22 A) but whether the observed microvilli belonged to these structures is yet to be confirmed.

4.3.3. Scaling of eyes with body size

When the number of facets, rhabdom and facet diameters were scaled against body length and head width it was observed that the main factor influencing the scaling of these sensory units was time of activity and not size (Figure 23). Size did play a role in the number of facets an animal possessed but the effects of time of activity are equally evident, particularly when considering the reduction in facet numbers in *N. ectatommoides* relative to the similarly sized *M. hirsutus* major workers (Figure 23 A, B). Two size metrics (BL and HW) were used for consistency but there was no major difference observed between them.

4.4. Discussion

There was a positive linear correlation between the eye area and body length (Figure 19). *Pheidole sp. 1* minors had the smallest body length and smallest eye areas (BL = 1.7mm, eye area = 6,722µm²) while *I. purpureus* was the largest in both respects (BL =8.7mm, eye area = 122,330µm²). The regression predicted eye area for most species fairly well, however, more data is necessary to confidently establish if species truly follow this pattern of scaling. One outlier was *Pheidole sp. 1* (major workers). Compared to the similarly sized *M. hirsutus* minor workers, *Pheidole sp. 1* majors had very small eyes (4.2 times smaller). This seems like a large amount of variation to see between species of such similar body size, so it seems reasonable to hypothesise that *Pheidole sp. 1* majors invest remarkably less in overall eye size than would be expected for their body size. If such a large amount of variation can be effected by differential investment it may not be possible to accurately predict eye area based on body length alone. Greater care must be taken to account for differences in the tasks that different ants perform.

The number of facets is in part dictated by the size of the eye and as a consequence, larger animals tended to have more facets. *Pheidole sp. 1* minor workers had the fewest facets (21) and *I. purpureus* had the most (496). However, when similarly sized animals occupying different temporal niches were compared it became apparent that time of activity also plays a role (Figure 23). Despite having similar body lengths the night-active *Pheidole sp. 1* majors have 9 times fewer facets than the day-active *M. hirsutus* minors. Meanwhile, the night-active *N. ectatommoides* (BL = 5.8mm) have 1.4 times fewer facets than the day-active *M. hirsutus* majors (BL = 5.4mm). This discrepancy between day- and night-active species indicates that the latter invest less in the number of facets per eye. This is consistent with previous findings by Menzi (1987). However, the difference from an increase

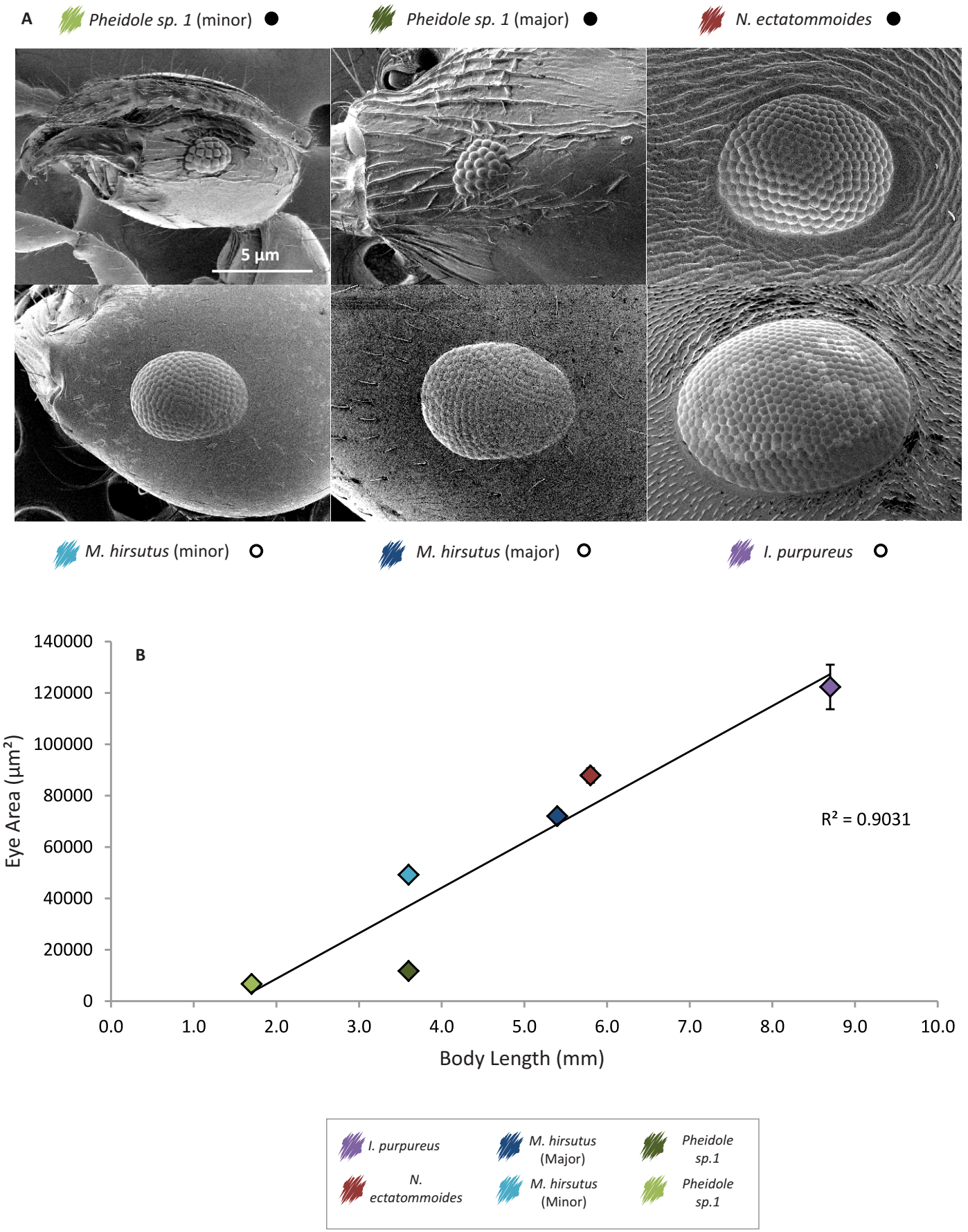

Figure 19

Summary of the eye structure of the six studied animals. **(A)** SEM images of the external morphology of the eyes of six animals. Top row: night-active animals (closed circles); bottom row: day-active animals (open circles). **(B)** Relation of eye area with body length of animals. Eye area was determined from cornea replicas (x̄±SE, n= 4). Note: errors bars in some cases may not be visible as the data is tightly packed. Regression line is shown by a continuous line.

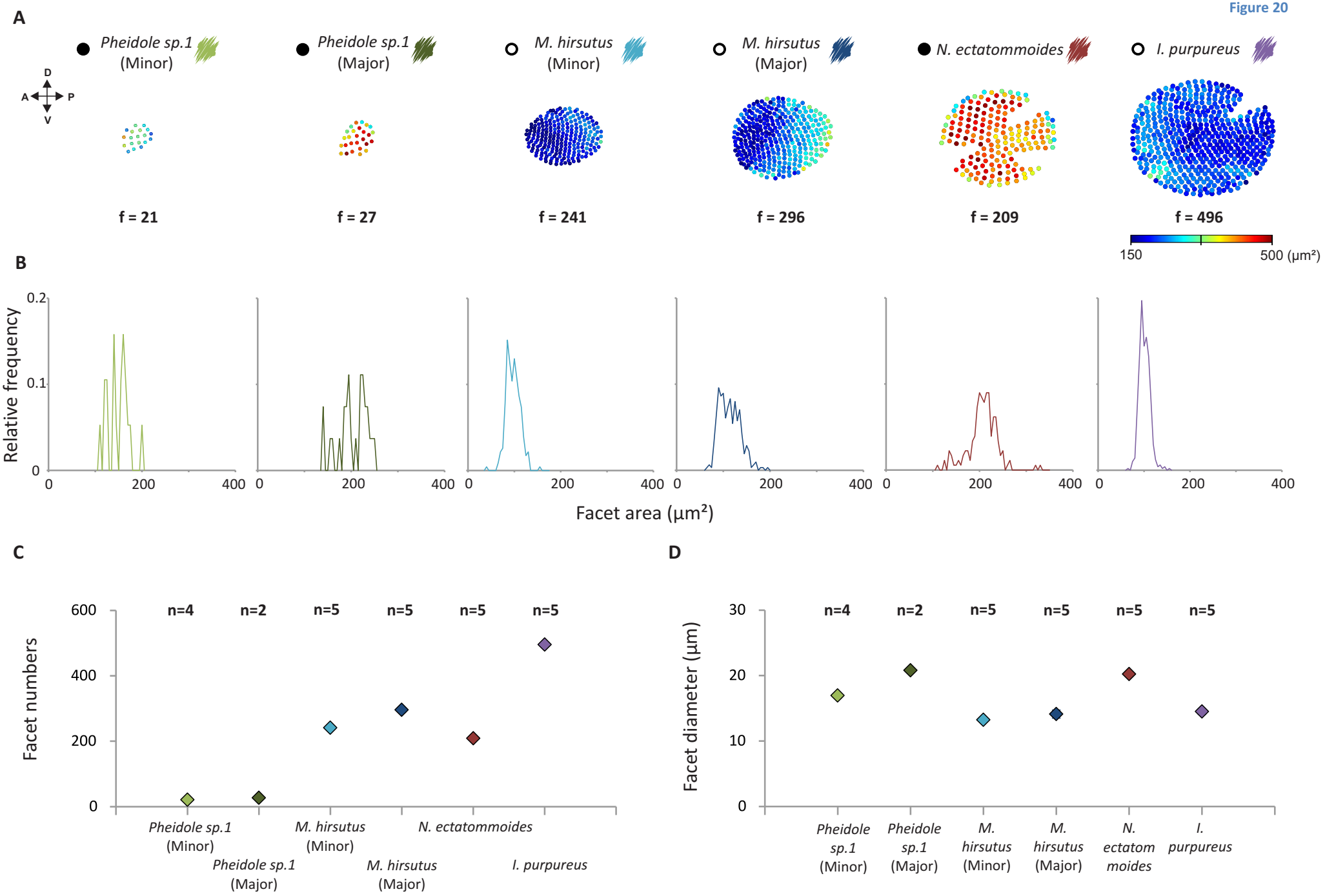
A
Pheidole sp.1 (Minor)
Pheidole sp.1 (Major)
M. hirsutus (Minor)
M. hirsutus (Major)
N. ectatommoides
I. purpureus
D
A
P
V
f = 21
f = 27
f = 241
f = 296
f = 209
f = 496
150
500 (µm²)
B
Relative frequency
0.2
0.1
0
0
200
400
Facet area (µm²)
C
Facet numbers
600
400
200
0
n=4
n=2
n=5
n=5
n=5
n=5
Pheidole sp.1 (Minor)
Pheidole sp.1 (Major)
M. hirsutus (Minor)
M. hirsutus (Major)
N. ectatommoides
I. purpureus
D
Facet diameter (µm)
30
20
10
0
n=4
n=2
n=5
n=5
n=5
n=5
Pheidole sp.1 (Minor)
Pheidole sp.1 (Major)
M. hirsutus (Minor)
M. hirsutus (Major)
N. ectatom moides
I. purpureus

Figure 20

Summary figure displaying results from facet replica mapping. **(A)** Facet maps from one worker of each species, warm colours (reds and yellows) represent larger facet areas (μm²) while cool colours (blues) represent smaller facet areas (see scale on right hand side). Dorsal, anterior, ventral and posterior directions for all eye maps are indicated on the left. Number of facets ("f") is given under each facet map. **(B)** The relative frequency distributions of facet areas are represented by individual histograms for each species (see colour codes next to species names at the top), larger species exhibit more regular, continuous distributions while *Pheidole sp. 1* major and minor workers have fairly erratic distributions due to the increased variability seen in this species (a characteristic trait of miniature species). **(C)** Average facet numbers ($\bar{x}$±SE, n = indicated on figure) and **(D)** average facet diameters for each species ($\bar{x}$±SE, n = 10 facets per individual with number of individuals indicated on figure), note the low number and large diameter of facets seen in night active species relative to day active ones. Note that error bars are shown for all data points but may be too close to the mean to be visible in some instances.

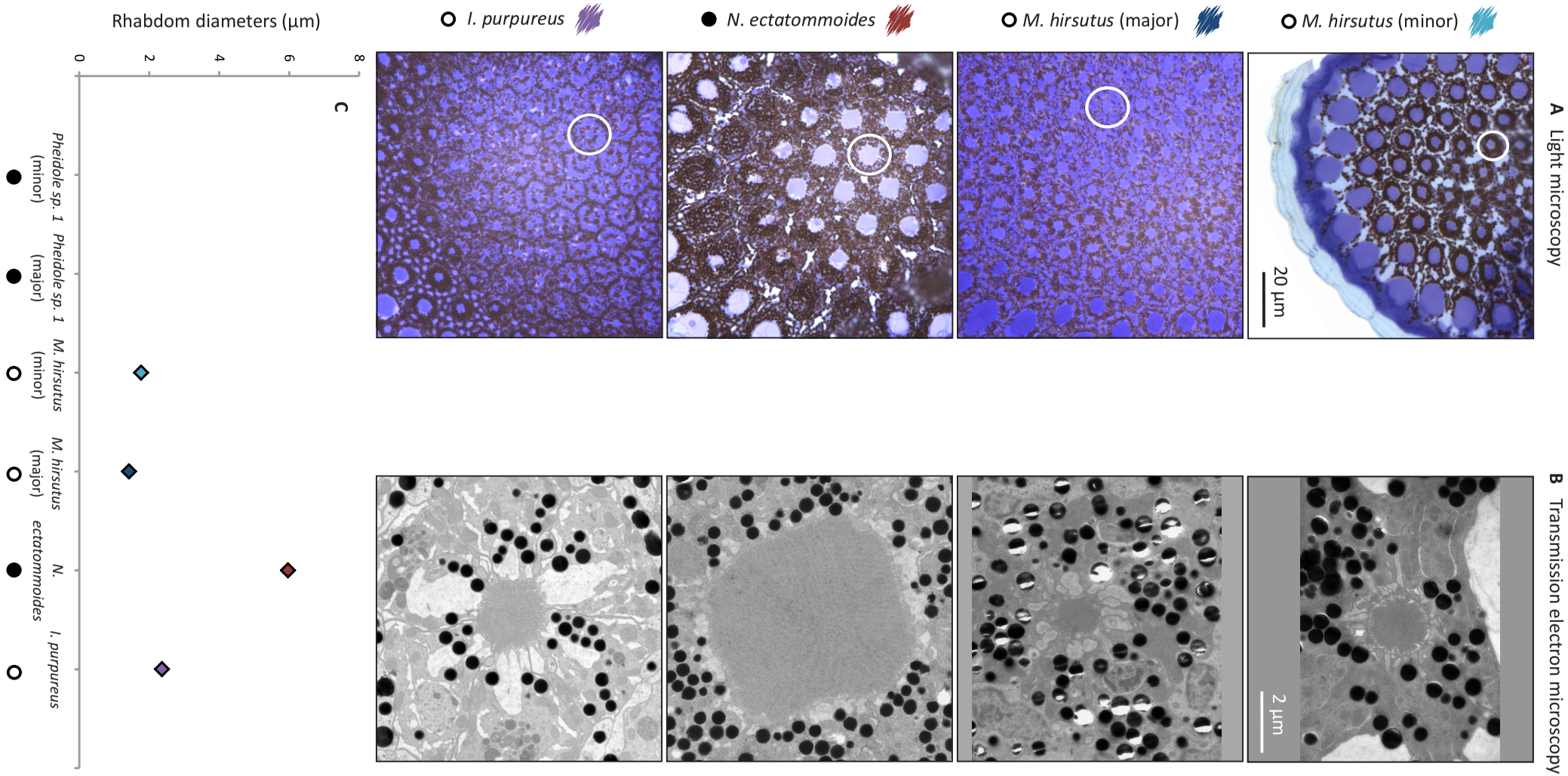

Figure 21

Internal structure of compound eye of four of the six different animals. **(A)** Light microscopy images of cross-sections of distal rhabdoms (circled). Rhabdoms are only seen here in the centre of the eye (upper left hand corner of each image) as at this level peripheral ommatidia are still at the level of the crystalline cone. **(B)** Transmission electron microscopy sections of individual rhabdoms. **(C)** Average rhabdom diameters (x̄±SE, n= 4). Note: errors bars in some cases may not be visible as the data is tightly packed. Unfortunately data for *Pheidole sp. 1* were not available. Night-active animals: closed circles; day-active animals: open circles.

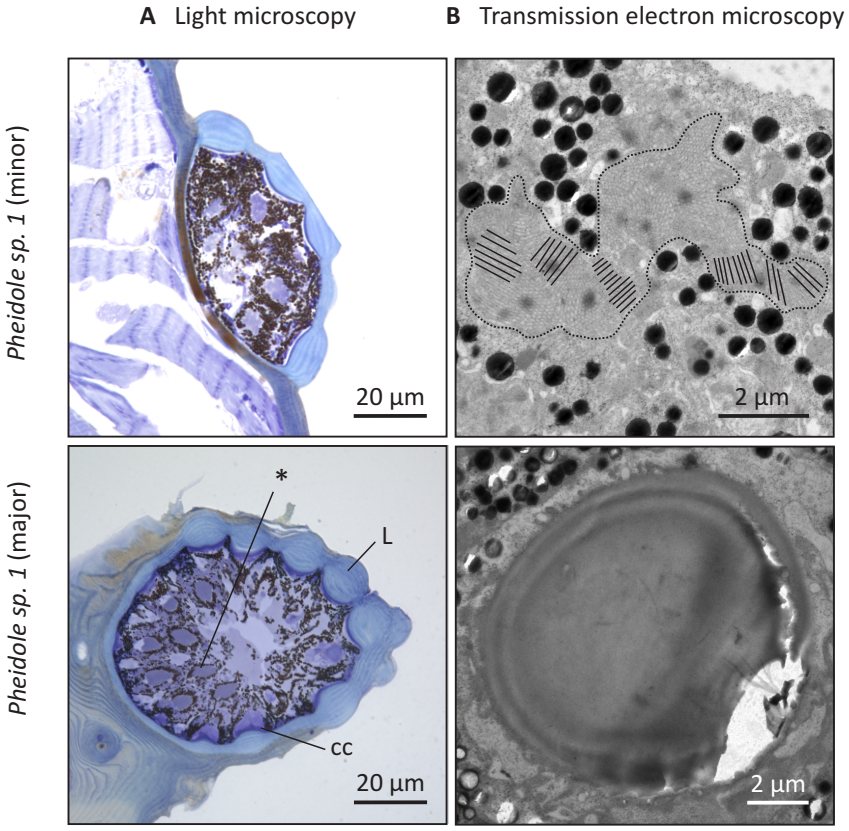

Figure 22

Preliminary observations of the internal structure of the compound eye of the small *Pheidole sp. 1* major and minor workers. **(A)** Light microscopy sections of the minor (top) and major worker (bottom). Labelled in the section are L = lens, cc = crystalline cone, * = putative rhabdom. **(B)** Transmission electron microscopy cross-sections of individual rhabdoms could not be collected but microvilli were observed in a convoluted pattern 'S' shaped pattern in a minor worker (top; outlined in dotted line). The microvilli orientation is indicated by line illustration as the orientation is difficult to discern from the image. The tip of a lens was captured in cross-section for a major worker (bottom).

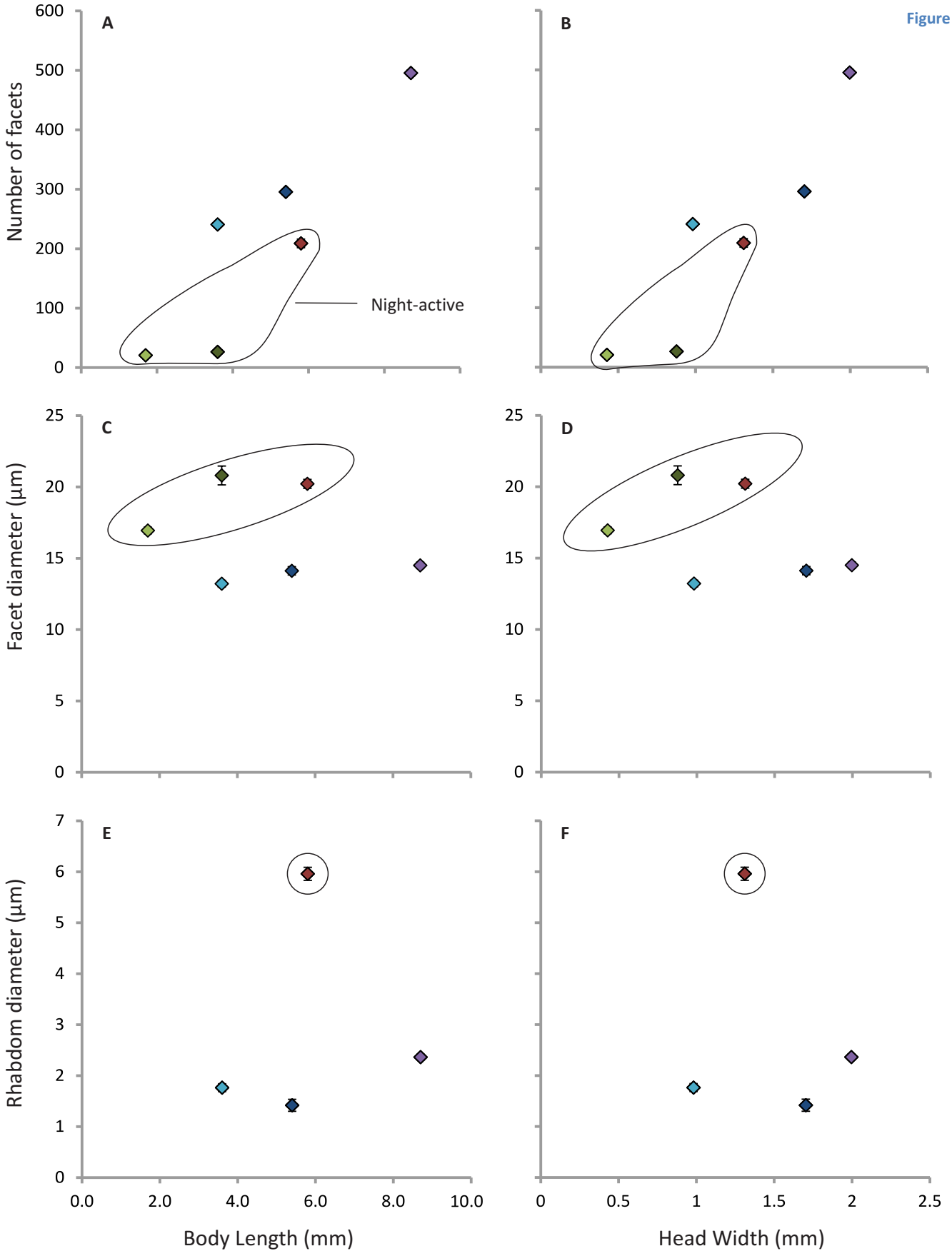

Iridomyrmex purpureus

Melophorus hirsutus (Major)

Pheidole sp.1 (Major)

Notoncus ectatommoides

Melophorus hirsutus (Minor)

Pheidole sp.1 (Minor)

Figure 23

Summary of changes to elements of the optic apparatus with changes to body size. Column one displays changes with respect to body length while column two relates the same changes to head width. (A) and (B) follow changes to the number of facets ($\bar{x}$±SE, n= 5); (C) and (D) track changes to facet diameters ($\bar{x}$±SE, n≥20); (E) and (F) illustrate the changes to rhabdom diameters ($\bar{x}$±SE, n= 4), unfortunately rhabdom data for Pheidole sp. 1 were not available. The time of day active is specified for each species by either open circles (Day active) or closed circles (Night active). Note that error bars are shown for all data points but may be too close to the mean to be visible in some instances.

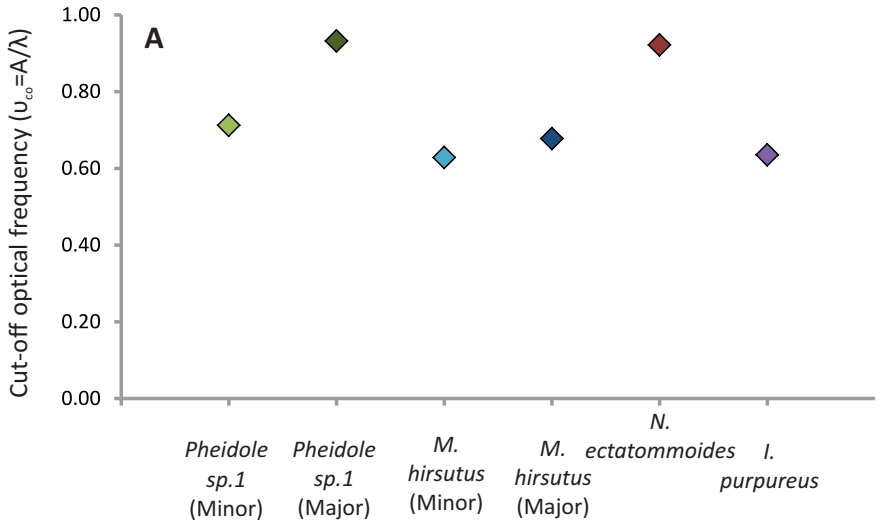
A
Cut-off optical frequency (υ_{co}=A/λ)
1.00
0.80
0.60
0.40
0.20
0.00
Pheidole sp.1 (Minor)
Pheidole sp.1 (Major)
M. hirsutus (Minor)
M. hirsutus (Major)
N. ectatommoides
I. purpureus

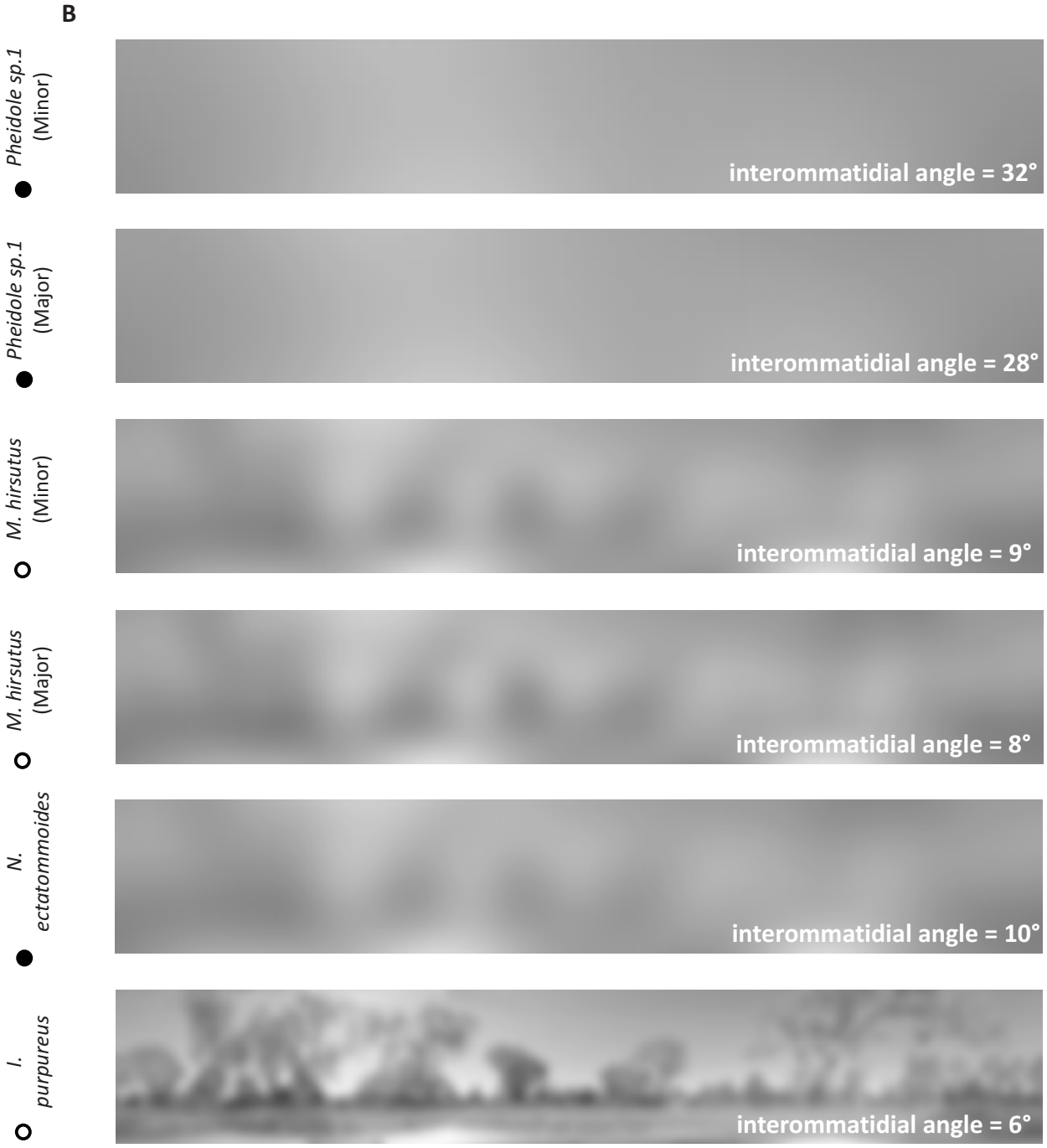
B
Pheidole sp.1 (Minor)
interommatidial angle = 32°
Pheidole sp.1 (Major)
interommatidial angle = 28°
M. hirsutus (Minor)
interommatidial angle = 9°
M. hirsutus (Major)
interommatidial angle = 8°
N. ectatommoides
interommatidial angle = 10°
I. purpureus
interommatidial angle = 6°

Figure 24

(A) Results from optical cut-off frequency calculations (figures given in λ = wavelength in μm) indicate that day active species tend to have better resolving power than night-active animals. However, these calculations do not take into account the number of facets in an array. **(B)** Simulations generated using a Gaussian blurring function (details given in methods section) give an indication of the spatial information available to different animals based on the number of facets they possess. Each image represents a panoramic natural scene spanning 360° horizontally and 55° vertically. Circles adjacent to species names indicate time of activity (open circles = day-active, closed circles = night-active).

by a factor of nine compared to an increase by a factor of 1.4 seems to go beyond natural variability between species and indicates a further reduction in investment in facet numbers by major workers of *Pheidole sp. 1.*

Unlike other factors described above the size of facets did not scale with body size. Time of activity was the driving factor in shaping facet size with night-active species having larger facets than their day-active counterparts (Figure 20). This is consistent with the findings of previous studies on ants and other related hymenopterans (Greiner et al., 2007, Narendra et al., 2011, Warrant and Dacke, 2011). Furthermore, given that the sensitivity of an eye is dependent on the absolute size of the optic elements it stands to reason that the facet diameter will always be dependent on the light capturing requirements of an animal independent of their size.

Night-active species increased the facet diameter even to the detriment of facet numbers. *N. ectatommoides* possess a larger eye area than *M. hirsutus* major yet has considerably fewer facets. Therefore it seems that night-active ants prioritise optical sensitivity (increasing facet diameter) over resolution (number of facets).

Rhabdom diameters did not scale with body size and this is reflected in Figure 23 E and F. Despite being 2.4 times larger in body length, *I. purpureus* had a very similar rhabdom diameter to that of the smallest species for which data is available, *M. hirsutus* minor (rhabdom diameter = 2.4 and 1.8 µm respectively). In contrast, the night-active *N. ectatommoides* had a rhabdom diameter 2.5 times greater than the day-active *I. purpureus* despite having a smaller body size. In addition, a previous study in ants of the genus *Myrmecia* observed similar rhabdom diameters in the nocturnal *M. pyriformis* major (rhabdom diameter = 5.9µm) than those seen in *N. ectatommoides* (rhabdom diameter = 6.0µm) even though *M. pyriformis* majors were five times larger than *N. ectatommoides* (Narendra et al., 2011). Similarly, the rhabdom diameters of the large, day-active species *Myrmecia croslandi* (rhabdom diameter = 1.3µm) were very similar to those observed in the *M. hirsutus* major workers (rhabdom diameter = 1.4µm) despite being 2.2 times larger. It is apparent that rhabdom diameters scale not with size but changes with visual sensitivity requirements as dictated by time of activity (Greiner et al., 2007, Narendra et al., 2011, Warrant and Dacke, 2011).

Across the various eye components examined, differences between *Pheidole sp. 1* major and minor workers were much more marked than those seen between *M. hirsutus* major and minor workers. Similar differences in the number and size of ommatidia between major and minor workers have been observed in the past by several studies (Baker and Ma, 2006, Klotz et al., 1992, Menzel and Wehner, 1970, Bernstein and Finn, 1971). These differences have been explained as a function of differential distribution of labour among worker castes. However, in past studies the major workers have always had significantly more and larger facets than the minor workers, with the former performing the more visually demanding tasks such as hunting and foraging while the latter specialised in digging and underground nest maintenance (Klotz et al., 1992, Menzel and Wehner, 1970). In this study it seems that the inverse is true of the labour allocation, in *Pheidole sp. 1* minor workers constitute the main foraging caste while major workers are relatively rare and seem to engage mainly in nest defence (personal observation FRE). Major workers do possess more and larger facets, although the difference in numbers is much less than what would be expected by comparing body size (see Figure 20 C).

Miniature animals are thought to endure high costs, particularly in the maintenance of metabolically expensive and disproportionately large nervous tissues (see Seid et al., 2011). This could partially explain the unexpectedly reduced size of the visual array seen in *Pheidole sp. 1* as the production of major workers may already possess a significant cost to a colony. Assuming that the tasks which major workers perform are not visually demanding, reducing the size of eyes and consequently the number of neurons necessary may lower the metabolic costs of maintaining such large animals within a colony, at least from the visual perspective.

Results from the optical cut-off frequency calculations based on maximum facet diameters indicate that day-active animals tend to have better resolving power than night-active animals (Figure 24 A). However, these calculations do not take into account the number of facets in an array. Simulations generated using a Gaussian blurring function (details given in methods section) gives an indication of the spatial information available to different animals based on the number of facets they possess (Figure 24 B). Neither of these approaches provide a full picture of the resolving power and spatial information available to an ant with a given set of eye characterisitics. Rather, the two approaches complement each other. To get a more complete idea of the visual capabilities, of an ant other calculations can be carried out to determine an animal's visual sensitivity, and behavioural and electrophysiological assays can be used to determine the spectral sensitivity of an animal. However, these were outside the scope of this study.

Most of the observed changes to the visual system were linked to time of activity rather than body size. However, the absolute size of an eye is still in part dictated by body size. An animal may invest less in vision and therefore reduce eye size relative to its body but the upper limit on the size of an eye still seems to be strongly linked to body size. This can lead to a severe limitation in the amount of visual information available to animals as seen in the case of *Pheidole sp. 1* major and minor workers. In cases as extreme as these, where the average number of facets is as low as 21 (*Pheidole sp. 1* minor workers), it is probable that the best an eye can hope to accomplish is to distinguish between light and dark areas. Given other animals' ability to move from one place to another using only photosensitive eye spots (Jekely et al., 2008), this may just be enough.

5. Conclusions

The aim of this study was to establish the effects of miniaturisation and time of activity on the design of chemoreceptive and visual systems in ants. To address this a comparative approach was employed: (1) four species of ants with body sizes ranging between 1.7mm to 8.7mm were selected, (2) the time of activity for the selected study species ranged from being strictly diurnal (2 species) to strictly nocturnal (2 species), (3) the external morphology and distribution of three chemosensory sensilla was studied using scanning electron micrographs, (4) the external and internal anatomy of compound eyes were studied using a variety of microscopy techniques. From these the variation in size, numbers and distribution of sensory units relative to body size and time of activity were established across the differently sized ants.

Of the four studied species, three had not been studied previously in the context of time of activity. New, detailed information on these species' activity schedules is presented here.

The study of the ant chemoreceptive system was centred around the external morphology of chemoreceptive sensilla, their size, abundance and distribution on the apical segment of the antennae. In this respect, this study is unique in being the first to record such detailed information on sensory sensilla. Although previous studies have carried out surveys of ant sensilla they usually have focused on identifying all the types of receptors that are present and report the total numbers per antennal segment, occasionally comparing variation between worker and reproductive castes (e.g. Dumpert, 1972b, Nakanishi et al., 2009, Renthal et al., 2003). The data collected here from detailed studies of SEM images revealed several previously unknown trends. Firstly, the number of sensilla was found to be strongly correlated to the apical segment area and less so to body length. This showed that the number of sensilla is primarily constrained by the size available on the antenna. Animals can and do increase the size of the apical segment area relative to body size, potentially to include more sensilla in their sensory array. The smallest animals had apical segment areas which were comparable to those of animals two to three times larger than themselves. This could mean that as animals become smaller sensillum bearing structures must become proportionally larger in order to function. Sensilla may require a certain amount of space to operate for two main reasons: (1) there may be a limit to how closely spaced sensilla can be before air flow between them becomes limited and thus ceases to deliver chemical stimuli (Koehl, 2001, Berg and Purcell, 1977), (2) there may be a limit to how far the volume of an antenna may be reduced before it hampers the nervous innervation of sensilla as well as delivery of oxygen (through tracheae) and nutrients (from haemolymph) (Schneider, 1964). If this is the case it may be possible to calculate the area and volume 'allocated' to each sensillum to compare how this changes across animals of different sizes. As animals decrease in size a plateau may be reached for apical segment size (surface area and volume) below which antennae are no longer able to function.

The size of sensilla tended to increase with body size in two of the three types of sensilla studied. This trend was not very strong because the size of sensilla varied considerably even within individuals. This variation seemed to be, at least in part explained by the position of sensilla relative to the tip of the apical segment: sensilla decreased in size closer to the tip and increased in size closer to the base of the apical segment. This trend was particularly marked in the smallest ants but may also be a feature of night-active species. Time of activity did not seem to play an important role

for the design of chemoreceptors. It did not seem to influence the number of sensilla but night-active species did seem to possess larger apical segments.

The study of ant compound eyes yielded several interesting results. Body size seems to strongly influence total eye area and at extremely small sizes must impose a limit to eye size. Eye area also limited the number and size of facets. This becomes particularly important for small night-active species. This is because time of activity plays a very important role on the design of eyes. Night-active animals must contend with a severely light limited environment. The way in which the nocturnal species dealt with this was by increasing the diameter of facets and rhabdoms to increase the probability of photon capture (increasing sensitivity). For small night-active animals with a small eye area this meant drastically reducing the number of facets sacrificing resolution in favour of sensitivity. Simulations, demonstrated that the amount of visual information available to animals with different size of facets is extremely limited. It was not clear whether animals with limited visual capabilities compensated by enhancing their chemoreceptive abilities by either increasing the number or size of sensilla.

In conclusion, both chemoreceptive arrays and visual systems were greatly influenced by changes in body size. However, the design of chemoreceptive arrays seemed to be relatively impervious to changes in time of activity. Conversely, vision was greatly affected by the diminishing light levels accompanying changes from day- to night-activity. Because of this the visual systems of extremely small, night-active animals suffered doubly. Their small size limited the size of eyes and the low light levels drove facets and rhabdoms to greater diameters to increase sensitivity. This severely limited the number of facets per eye which incurred a great cost in terms of resolution. It appears that vision in these animals is extremely limited and may serve only as a rough means of orienting using patches of light and dark. It is very likely that in this situation animals may turn to chemoreception for additional information about their environment. This is supported by the increase in relative size of the apical segment in the smallest animals and the well-developed chemosensory arrays they possess. It is likely that an increased dependence on pheromone trail-following and general use of chemical cues accompanies this increase in investment on chemosensory structures. This presents an interesting new avenue of study which should shed more light on this fascinating phenomenon of miniaturisation.

References

ALTNER, H. & PRILLINGER, L. 1980. Ultrastructure of invertebrate chemo-, thermo-, and hygroreceptors and its functional significance. *International Review of Cytology,* 67**,** 69-139.

BAKER, G. T. & MA, P. W. K. 2006. Morphology and number of ommatidia in the compound eyes of *Solenopsis invicta*, *Solenopsis richteri,* and their hybrid (Hymenoptera: Formicidae). *Zoologischer Anzeiger,* 245**,** 121-125.

BERG, H. C. & PURCELL, E. M. 1977. Physics of chemoreception. *Biophysical Journal,* 20**,** 193-219.

BERNSTEIN, S. & FINN, C. 1971. Ant compound eye: size-related ommatidium differences within a single wood ant nest. *Experientia,* 27**,** 708-710.

BEUGNON, G., CHAGNÉ, P. & DEJEAN, A. 2001. Colony structure and foraging behavior in the tropical formicine ant, *Gigantiops destructor*. *Insectes Sociaux,* 48**,** 347-351.

BRUNNERT, A. & WEHNER, R. 1973. Fine structure of light- and dark-adapted eyes of desert ants, *Cataglyphis bicolor* (Formicidae, Hymenoptera). *Journal of Morphology,* 140**,** 15-29.

CHITTKA, L. & NIVEN, J. 2009. Are bigger brains better? *Current Biology,* 19**,** R995-R1008.

CHITTKA, L. & SKORUPSKI, P. 2011. Information processing in miniature brains. *Proceedings of the Royal Society B: Biological Sciences,* 278**,** 885-888.

CHRISTIANSEN, P. 2002. Locomotion in terrestrial mammals: the influence of body mass, limb length and bone proportions on speed. *Zoological Journal of of the Linnean Society,* 136**,** 685-714.

COLE, B. J. 1985. Size and behavior in ants: constraints on complexity. *Proceedings of the National Academy of Sciences,* 82**,** 8548-8551.

COLLETT, M. & COLLETT, T. S. 2000. How do insects use path integration for their navigation? *Biological Cybernetics,* 83**,** 245-259.

DE GROOT, R. 1983. Origin, status and ecology of the owls in Galapagos. *Ardea,* 71**,** 167-182.

DUMPERT, K. 1972a. Alarmstoffrezeptoren auf der Antenne von *Lasius fuliginosus* (Latr.)(Hymenoptera, Formicidae). *Journal of Comparative Physiology A: Neuroethology, Sensory, Neural, and Behavioral Physiology,* 76**,** 403-425.

DUMPERT, K. 1972b. Bau und verteilung der sensillen auf der antennengeißel von *Lasius fuliginosus* (Latr.)(Hymenoptera, Formicidae). *Zoomorphology,* 73**,** 95-116.

EBERHARD, W. G. 2007. Miniaturized orb-weaving spiders: behavioural precision is not limited by small size. *Proceedings of the Royal Society B: Biological Sciences,* 274**,** 2203-2209.

EGUCHI, E. & TOMINAGA, Y. (eds.) 1999. *Atlas of arthropod sensory receptors: Dynamic morphology in relation to function* Tokyo: Springer-Verlag.

ESQUIVEL, F. 2011. Identification and distribution of antennal sensory sensilla of *Myrmecia pyriformis* (Hymenoptera: Formicidae). *ANU BIOL3138 Special Topics*

FRAZIER, J. L. 1985. Nervous system: Sensory system. *In:* BLUM, M. S. (ed.) *Fundamentals of Insect Physiology.* New York: Wiley-Interscience.

GREENAWAY, P. 1981. Temperature limits to trailing activity in the australian arid-zone meat ant *Iridomyrmex purpureus* form *viridiaeneus*. *Australian Journal of Zoology,* 29**,** 621-630.

GREINER, B., NARENDRA, A., REID, S. F., DACKE, M., RIBI, W. A. & ZEIL, J. 2007. Eye structure correlates with distinct foraging-bout timing in primitive ants. *Current Biology,* 17**,** R879-R880.

GRUBB JR, T. C. 1978. Weather-dependent foraging rates of wintering woodland birds. *The Auk***,** 370-376.

HANKEN, J. & WAKE, D. B. 1993. Miniaturization of body size: organismal consequences and evolutionary significance. *Annual Review of Ecology and Systematics,* 24**,** 501-519.

HANSSON, BILL S. & STENSMYR, MARCUS C. 2011. Evolution of insect olfaction. *Neuron,* 72**,** 698-711.

HASHIMOTO, Y. 1990. Unique features of sensilla on the antennae of Formicidae (Hymenoptera). *Applied Entomology and Zoology,* 25**,** 491-501.

HÖLLDOBLER, B. & WILSON, E. O. 1990. *The Ants,* Cambridge, Massachusetts, The Belknap Press of Harvard University Press.

HONE, D. W. E. & BENTON, M. J. 2005. The evolution of large size: how does Cope's Rule work? *Trends in Ecology & Evolution,* 20**,** 4-6.
JEKELY, G., COLOMBELLI, J., HAUSEN, H., GUY, K., STELZER, E., NEDELEC, F. & ARENDT, D. 2008. Mechanism of phototaxis in marine zooplankton. *Nature,* 456**,** 395-399.
KLEINEIDAM, C., ROMANI, R., TAUTZ, J. & ISIDORO, N. 2000. Ultrastructure and physiology of the CO2 sensitive sensillum ampullaceum in the leaf-cutting ant *Atta sexdens*. *Arthropod Structure and Development,* 29**,** 43-55.
KLEINEIDAM, C. & TAUTZ, J. 1996. Perception of carbon dioxide and other “air-condition” parameters in the leaf cutting ant *Atta cephalotes*. *Naturwissenschaften,* 83**,** 566-568.
KLOTZ, J. H., REID, B. L. & GORDON, W. C. 1992. Variation of ommatidia number as a function of worker size in *Camponotus pennsylvanicus* (DeGeer) (Hymenoptera: Formicidae). *Insectes Sociaux,* 39**,** 233-236.
KOEHL, M. A. R. 2001. Fluid dynamics of animal appendages that capture molecules: arthropod olfactory antennae. *In:* FAUCI, L. J. & GUERON, S. (eds.) *Computational Modeling in Biological Fluid Dynamics.* New York: Springer Verlag.
KOHLER, M. & WEHNER, R. 2005. Idiosyncratic route-based memories in desert ants, *Melophorus bagoti*: how do they interact with path-integration vectors? *Neurobiology of Learning and Memory,* 83**,** 1-12.
KOTLER, B. P., BROWN, J. S. & HASSON, O. 1991. Factors affecting gerbil foraging behavior and rates of owl predation. *Ecology***,** 2249-2260.
KRONFELD-SCHOR, N. & DAYAN, T. 2003. Partitioning of time as an ecological resource. *Annual Review of Ecology, Evolution, and Systematics,* 34**,** 153-181.
LAND, M. F. 1997. Visual acuity in insects. *Annual Review of Entomology,* 42**,** 147-177.
MANILOFF, J. 1996. The minimal cell genome: "On being the right size". *Proceedings of the National Academy of Sciences USA,* 93**,** 10004-10006.
MARQUES-SILVA, S., MATIELLO-GUSS, C. P., DELABIE, J. H. C., MARIANO, C. S. F., ZANUNCIO, J. C. & SERRÃO, J. E. 2006. Sensilla and secretory glands in the antennae of a primitive ant: *Dinoponera lucida* (Formicidae: Ponerinae). *Microscopy research and technique,* 69**,** 885-890.
MCIVER, S. B. 1975. Structure of cuticular mechanoreceptors of arthropods. *Annual Review of Entomology,* 20**,** 381-397.
MENZEL, R. & WEHNER, R. 1970. Augenstrukturen bei verschiedengroβen Arbeiterinnen von *Cataglyphis bicolor* Fabr. (Formicidae, Hymenopetera). *Zeitschrift fur Vergleichende Physiologie,* 68**,** 446-449.
MENZI, U. 1987. Visual adaptation in nocturnal and diurnal ants. *Journal of Comparative Physiology A,* 160**,** 11-21.
MOSER, J. C., REEVE, J. D., BENTO, J., EACUTE, MAUR, IACUTE, S., C., DELLA LUCIA, T., C., N. M., CAMERON, R. S. & HECK, N. M. 2004. Eye size and behaviour of day- and night-flying leafcutting ant alates. *Journal of Zoology,* 264**,** 69-75.
NAKANISHI, A., NISHINO, H., WATANABE, H., YOKOHARI, F. & NISHIKAWA, M. 2009. Sex-specific antennal sensory system in the ant *Camponotus japonicus*: structure and distribution of sensilla on the flagellum. *Cell and Tissue Research,* 338**,** 79-97.
NARENDRA, A. 2007. Homing strategies of the Australian desert ant *Melophorus bagoti* II. Interaction of the path integrator with visual cue information. *Journal of Experimental Biology,* 210**,** 1804-1812.
NARENDRA, A., REID, S. F., GREINER, B., PETERS, R. A., HEMMI, J. M., RIBI, W. A. & ZEIL, J. 2011. Caste-specific visual adaptations to distinct daily activity schedules in Australian *Myrmecia* ants. *Proceedings of the Royal Society B: Biological Sciences,* 278**,** 1141-1149.
NARENDRA, A., REID, S. F. & HEMMI, J. M. 2010. The twilight zone: ambient light levels trigger activity in primitive ants. *Proceedings of the Royal Society B: Biological Sciences,* 277**,** 1531-1538.

NIVEN, J. E., ANDERSON, J. C. & LAUGHLIN, S. B. 2007. Fly photoreceptors demonstrate energy-information trade-offs in neural coding. *PLoS Biol,* 5**,** e116.
NIVEN, JEREMY E. & FARRIS, SARAH M. 2012. Miniaturization of nervous systems and neurons. *Current Biology,* 22**,** R323-R329.
NIVEN, J. E. & LAUGHLIN, S. B. 2008. Energy limitation as a selective pressure on the evolution of sensory systems. *Journal of Experimental Biology,* 211**,** 1792-1804.
OLMO, E. 1983. Nucleotype and cell size in vertebrates: a review. *Basic and applied histochemistry,* 27**,** 227-256.
OZAKI, M., WADA-KATSUMATA, A., FUJIKAWA, K., IWASAKI, M., YOKOHARI, F., SATOJI, Y., NISIMURA, T. & YAMAOKA, R. 2005. Ant nestmate and non-nestmate discrimination by a chemosensory sensillum. *Science's STKE,* 309**,** 311.
PIRIE, N. W. 1973. "On Being the Right Size". *Annual Review of Microbiology,* 27**,** 119-132.
PROVOST, E., BLIGHT, O., TIRARD, A AND RENUCCI, M. 2008. *Hydrocarbons and insects' social physiology*, Nova Science Publishers, Inc.
REID, S. F., NARENDRA, A., HEMMI, J. M. & ZEIL, J. 2011. Polarised skylight and the landmark panorama provide night-active bull ants with compass information during route following. *Journal of Experimental Biology,* 214**,** 363-370.
RENSCH, B. 1948. Histological changes correlated with evolutionary changes of body size. *Evolution,* 2**,** 218-230.
RENTHAL, R., VELASQUEZ, D., OLMOS, D., HAMPTON, J. & WERGIN, W. P. 2003. Structure and distribution of antennal sensilla of the red imported fire ant. *Micron,* 34**,** 405-413.
RIBI, A., ENGELS, E. & ENGELS, W. 1989. Sex and caste specific eye structures in stingless bees and honeybees (Hymenoptera: Trigonidae, Apidae). *Entomologia Generalis,* 14**,** 233-242.
ROTH, G., ROTTLUFF, B., GRUNWALD, W., HANKEN, J. & LINKE, R. 1990. Miniaturization in plethodontid salamanders (Caudata: Plethodontidae) and its consequences for the brain and visual system. *Biological Journal of the Linnean Society,* 40**,** 165-190.
RUTCHY, M., ROMANI, R., KUEBLER, L. S., RUSCHIONI, S., ROCES, F., ISIDORO, N. & KLEINEIDAM, C. J. 2009. The thermo-sensitive sensilla coeloconica of leaf-cutting ants (*Atta vollenwenderi*). *Arthropod Structure and Development,* 38**,** 195-205.
RYAN, M. F. 2002. *Insect chemoreception,* Dordrecht, Kluwer Academic Publishers.
SCHNEIDER, D. 1964. Insect antennae. *Annual Review of Entomology,* 9**,** 103-122.
SCHOENER, T. W. 1974. Resource partitioning in ecological communities. *Science* 185**,** 27-39.
SCHWARZ, S., ALBERT, L., WYSTRACH, A. & CHENG, K. 2011. Ocelli contribute to the encoding of celestial compass information in the Australian desert ant *Melophorus bagoti*. *Journal of Experimental Biology,* 214**,** 901-906.
SEID, M. A., CASTILLO, A. & WCISLO, W. T. 2011. The allometry of brain miniaturization in ants. *Brain, Behavior and Evolution,* 77**,** 5-13.
STEINBRECHT, R. A. 1999. Olfactory Receptors. *In:* EGUCHI, E., TOMINAGA, Y. (ed.) *Atlas of arthropod sensory receptors.* Tokyo: Springer-Verlag.
VICKERS, N. 2000. Mechanisms of animal navigation in odor plumes. *The Biological Bulletin,* 198**,** 203-212.
WARD, P. S. & BRADY, S. G. 2003. Phylogeny and biogeography of the ant subfamily Myrmeciinae (Hymenoptera: Formicidae). *Invertebrate Systematics,* 17**,** 605-605.
WARRANT, E. & DACKE, M. 2011. Vision and visual navigation in nocturnal insects. *Annual Review of Entomology,* 56**,** 239-254.
WARRANT, E. & NILSSON, D.-E. (eds.) 2006. *Invertebrate vision,* Cambridge: Cambridge University Press.
WEHNER, R., FUKUSHI, T. & ISLER, K. 2007. On being small: brain allometry in ants. *Brain, Behavior and Evolution,* 69**,** 220-228.
WEHNER, R., MICHEL, B. & ANTONSEN, P. 1996. Visual navigation in insects: coupling of egocentric and geocentric information. *Journal of Experimental Biology,* 199**,** 129-40.

WEHNER, R. & SRINIVASAN, M. V. 2003. Path integration in insects. *In:* JEFFREY, K. K. (ed.) *The neurobiology of spatial behaviour.* Oxford: Oxford University Press.
WELBERGEN, J. A. 2008. Variation in twilight predicts the duration of the evening emergence of fruit bats from a mixed-species roost. *Animal Behaviour,* 75**,** 1543-1550.
WICHER, D. 2012. Functional and evolutionary aspects of chemoreceptors. *Frontiers in Cellular Neuroscience,* 6.
WILSON, E. O. 1972. *The Insect Societies,* Cambridge, Massachusetts, The Belknap Press of Harvard University Press.
WILSON, E. O. 2003. *Pheidole in the new world: a dominant, hyperdiverse ant genus,* Cambridge, Harvard University Press.
WITTLINGER, M., WEHNER, R. & WOLF, H. 2007. The desert ant odometer: a stride integrator that accounts for stride length and walking speed. *Journal of Experimental Biology,* 210**,** 198-207.
WOODWARD, G., EBENMAN, B., EMMERSON, M., MONTOYA, J. M., OLESEN, J. M., VALIDO, A. & WARREN, P. H. 2005. Body size in ecological networks. *Trends in Ecology & Evolution,* 20**,** 402-409.
ZACHARUK, R. Y. 1980. Ultrastructure and function of insect chemosensilla. *Annual Review of Entomology,* 25**,** 27-47.
ZEIL, J. 1983. Sexual dimorphism in the visual system of flies: The compound eyes and neural superposition in Bibionidae (Diptera). *Journal of Comparative Physiology A,* 150**,** 379-393.
ZEIL, J. 2012. Visual homing: an insect perspective. *Current Opinion in Neurobiology,* 22**,** 285-293.